Adiponectin Expression and Oxidative Stress in Hearts of Mice Fed a High-Fat Diet

by

Teresa Gorman

A thesis submitted to the Graduate Faculty of
Auburn University
in partial fulfillment of the
requirements for the Degree of
Master of Science

Auburn, Alabama
August 3, 2013

Keywords: obesity, cardiovascular disease, oxidative stress, reactive oxygen species, antioxidant, adiponectin

Approved by

Dean Schwartz, Chair, Associate Professor of Anatomy, Physiology, Pharmacology
Robert Judd, Associate Professor of Anatomy, Physiology, Pharmacology
Robert Kemppainen, Professor of Anatomy, Physiology, Pharmacology
Juming Zhong, Associate Professor of Anatomy, Physiology, Pharmacology

Abstract

Evidence suggests that excess superoxide generation leading to oxidative stress and/or the reduced capacity of organisms to regulate oxidative/redox environments play a major role in the initiation and progression of obesity related diseases. Oxidative stress contributes to the progression of numerous diseases throughout the body, including the cardiovascular system. Adiponectin is a protein hormone previously thought to be secreted only from adipose tissue. Adiponectin is generally lower in obese individuals and has been shown to play a cardio protective role. The purpose of our study was to examine the effects of niacin on antioxidant gene expression and activity in hearts of a mouse model of obesity and to also look at expression of adiponectin in the mouse heart, which could lead to a better understanding of adiponectin regulation and its role in cardiovascular and metabolic diseases.

Mice were fed high fat (60% kcal as fat) or normal diets for 11 weeks (10% kcal fat) as part of a separate study. Niacin was added to the drinking water to half of the mice for the last 5 weeks. At the end of the study, hearts were rapidly frozen in liquid nitrogen for the determination of sirtuins (SIRT), glutathione peroxidase (Gpx-1), superoxide dismutase-1 (SOD1), and superoxide dismutase-2 SOD2 gene expression, superoxide dismutase activity, and protein carbonylation. Mice fed the high fat diet had significantly increased body weights ($p<0.001$). There was no change in antioxidant

gene expression between the four groups and no sign of protein carbonylation, an oxidative stress marker, in the high-fat diet group compared to the control group. Increase in gene expression of SIRT1 and SIRT5 was seen in the high fat diet compared to normal diet. Niacin fed groups had an increase in SIRT1 protein expression compared to the groups without niacin. Real-time PCR showed expression of adiponectin in the mouse heart, with a slight increase of expression in the high-fat diet compared to control. Western blot analysis of adiponectin showed that adiponectin protein expression was significantly lowered in the high-fat diet compared to the control diet ($p<0.05$).

Mice on a high fat diet for 11 weeks did not show alterations in antioxidant gene expression, SOD activity, or protein carbonylation compared to control group. These results suggest that an 11 week high-fat diet was not a long enough period to induce significant oxidative stress on the mouse heart. Increases in mRNA expression of SIRT1 and SIRT5 in the high-fat and niacin diets, and increased SIRT1 protein expression in niacin fed hearts could be due to a protective role against oxidative stress.

Western blot and RT-PCR analysis show protein and mRNA expression of adiponectin in the mouse heart, and could potentially be eliciting a local response, along with circulating adiponectin. The type of tissue or cells in the heart expressing adiponectin is unknown and future studies examining adiponectin in isolated mouse myocytes could provide insight on which area of the heart is producing adiponectin.

Acknowledgements

I am extremely thankful for my advisor, Dr. Dean Schwartz, and I am grateful for his continual support, guidance and encouragement. I would also like to thank Dr. Robert Judd for his support and generosity of numerous resources and materials, and Dr. Robert Kemppainen and Dr. Juming Zhong for their supervision and help along the way.

Table of Contents

List of Tables

List of Figures

List of Abbreviations

CAT	Catalase
C/EBPα	CCAAT-enhancer-binding proteins
CGD	Chronic granulomatous disease
CVD	Cardiovascular disease
DsbA-L	Disulfide-bond A oxidoreductase-like protein
ER	Endoplasmic reticulum
ETC	Electron Transport Chain
GPx-1	Glutathione peroxidase-1
NOS	Nitric oxide synthase
NOX	NADPH oxidase
PPARγ	Peroxisome proliferator-activated receptor γ
ROS	Reactive oxygen species
SIR2	Silence information regulator 2
SIRT	Silent mating type information regulation
SOD	Superoxide dismutase
SOD1	Superoxide dismutase-1
SOD2	Superoxide dismutase-2
SOD3	Superoxide dismutase-3
TNFα	Tumor necrosis factor alpha

VLDL	very low-density lipoproproteins
XO	Xanthine oxidase

Literature Review

Cardiovascular disease (CVD) is the leading cause of death in the United States and worldwide [1, 2], with approximately 17 million deaths per year [3]. CVD is defined as any disease that affects the heart or blood vessels. Although the incidence of CVD has plateaued over the past ten years, CVD is still alarmingly prevalent in the United States. There are many factors that contribute to CVD including age, gender, genetics, and obesity [4]. Of these factors, obesity is at epidemic levels in the United States, and there is a strong correlation between obesity and CVD [5]. Obesity is a medical condition in which excess body fat accumulates to the extent that it may lead to reduced life expectancy and increased health problems, such as type 2 diabetes, certain types of cancer, high blood pressure, and other heart related diseases [6]. Studies show that obesity is also an independent risk factor for the development of heart disease and heart failure [7]. Research suggests that an increase in oxidative stress due to obesity contributes to the early stages of heart dysfunction [8].

Oxidative stress occurs when the amount of oxidants or reactive oxygen species (ROS) produced exceeds the amount of antioxidants available to detoxify these reactive intermediates. This can occur from an excessive generation of ROS or a lack of antioxidants. Oxidative stress is a contributing factor in the progression of numerous diseases including stroke [9], hypertension [10], diabetes mellitus [11],

neurodegeneration [12], aging [13], and CVD [14]. Because oxidative stress plays a role in the progression of such a large number and wide variety of diseases, it is important to understand the components and mechanisms of this pathway.

ROS are oxygen-derived molecules, which can be oxygen radicals like superoxide anion (O_2^-), hydroxyl radicals (OH), and peroxyl (RO_2), or non-radicals such as hydrogen peroxide (H_2O_2). ROS are generated under normal conditions as a consequence of aerobic metabolism. They are a particularly short-lived species due to their high chemical reactivity, and excessive ROS accumulation can lead to the reaction with, and subsequent alterations of DNA, proteins, carbohydrates, and lipids [15]. The alterations may ultimately lead to irreversible damage of these molecules and result in damage to biological systems.

There are many sources of ROS. Cellular production of ROS can occur by enzymatic or non-enzymatic pathways. Non-enzymatic ROS generation originates primarily from mitochondrial sources, especially from complex I and III in the electron transport chain (ETC). Electrons are transferred through the ETC, generating a proton gradient that drives the synthesis of ATP [16]. Some of the electrons passing through the mitochondrial ETC leak out and reduce molecular oxygen to form superoxide [17]. It has been reported that a 1-2% of O_2 consumption during normal respiration undergoes an electron reduction, generating superoxide [18]. Other types of ROS that can be generated are hydrogen peroxide (H_2O_2) and the hydroxyl free radical. The accumulation of these ROS can cause increased amounts of oxidative stress [19].

Along with the mitochondria, the endoplasmic reticulum (ER) and nuclear membrane are two examples of organelles that have enzymes capable of generating

free radicals. Both organelles have a strong correlation to redox cellular homeostasis, which is a factor in many diseases [20]. Nuclear membranes contain cytochrome oxidase enzymes that can generate superoxide. The ER is primarily involved in lipid and protein synthesis and plays a key role in protein folding and modification as well as in storage of calcium. Specifically, the smooth ER contains enzymes like cytochrome P-450 that oxidize unsaturated fatty acids and reduce molecular oxygen to superoxide [21].

An example of a ROS generating enzyme is Nitric oxide synthase (NOS). NOS regulates vascular tone [22], neurotransmission [23] and inflammation [24]. NOS catalyzes the production of nitric oxide (NO) from L-arginine [25]. There are three subtypes of NOS; the inducible form of NOS (iNOS), endothelial NOS (eNOS), and neuronal NOS (nNOS) [24]. INOS is involved in inflammation and cardioprotection. ENOS is expressed in endothelial cells and the NO generated from eNOS is involved in vascular tone [2]. NNOS is produced in nervous tissue and various other cell types and performs a role in cell communication [26].

Another enzyme capable of generating ROS is xanthine oxidase (XO), which is commonly used to study the effects of ROS on cellular processes [15]. XO catalyzes the conversion of hypoxanthine and xanthine to uric acid and generates hydrogen peroxide as a by-product [27]. XO can also create superoxide from xanthine dehydrogenase when exposed to hypoxia [21]. XO has been shown to play a role in vascular injury associated with ischemia, inflammatory diseases and chronic heart failure [28]. Other enzymatic sources of ROS include lipoxygenases, cyclooxgenases, and NADPH oxidase [15].

In addition to the damaging effects of ROS, these molecules can also exert beneficial effects. One important role of ROS is in the function of the immune system. The first study documenting the significance of ROS in immune function reported that there was a correlation between the generation of ROS and the ability of the patients' leukocytes to fight off pathogens [29]. The decreased ability of leukocytes to fight off invading pathogens is known as chronic granulomatous disease (CGD). CGD is a rare disease that was discovered in young boys suffering from repeated infections caused by the absence of the cytochrome b558 complex in phagocytes [30]. This complex is now called NADPH oxidase (NOX). NOX catalyzes this process and is necessary for the bacterial action of phagocytes [31].

NOX was originally discovered in neutrophils [32], and has the capacity to produce large amounts of superoxide. NOX is a membrane-bound enzyme that transports electrons across biological membranes to molecular oxygen and catalyzes the formation of superoxide. NOX is an important contributor to oxidative stress in the heart [33]. NOX has seven homologues named NOX1-5 and DOUX 1-2. Endothelial cells and cardiomyocytes generally express NOX2 and NOX4, while vascular smooth muscle cells express NOX4 [34], [35].

ROS also play a role in cell signaling that can be advantageous to the body. This type of cell signaling is referred to as "redox signaling," a process in which physiological levels of ROS induce changes to proteins that are discrete, site-specific, and reversible [36]. ROS are highly reactive and are formed and degraded very quickly, making them good second messengers in cellular signaling. Numerous cell types have been found to generate ROS through growth factors and cytokines [37]. These reactions require ROS

to regulate signaling cascades that can involve cell growth factors, cytokines, cell differentiation, and apoptosis [21]. Exogenous addition of superoxide or hydrogen peroxide has been shown to stimulate cell growth and differentiation in neuronal cells [38], cardiac cells [39], endothelial cells [40], fibroblasts [41], smooth muscle cells [42], and cancer cells [43]. These studies emphasize the importance of ROS for normal cell function.

Antioxidants and Oxidative Stress Markers

Antioxidants inhibit the oxidation or reactions promoted by oxygen, peroxides, or free radicals and can prevent oxidation of nucleic acids, proteins, and lipids. Normally, antioxidants decrease ROS by donating an electron to a free radical. Antioxidant defenses can occur endogenously or exogenously, and includes three general types of endogenous antioxidant defense. The first type is antioxidant proteins, including albumin, haptoglobin, ferritin, and ceruloplasmin, all of which are mostly found in the plasma [44, 45]. Protein antioxidants can function in numerous ways. For example, albumin has been shown to respond to stress by eliciting an antioxidant response, and haptoglobin binds free hemoglobin, which results in the inhibition of iron-induced oxidative damage [44-46]. The second type of endogenous antioxidants are small molecule antioxidants, including vitamin c, uric acid, bilirubin, glutathione, β-carotene, coenzyme Q10, and lycopene. The third type is enzymatic antioxidants, including superoxide dismutase (SOD), glutathione peroxidase-1 (GPX-1), and catalase (CAT).

These enzymes are produced in most mammalian cells and are good indicators of levels of cellular oxidative stress.

Excessive amounts of reactive oxygen species, especially superoxide, have been implicated in the pathogenesis of many cardiovascular diseases. Since the vascular levels of superoxide are regulated by SOD, the role of SOD in CVD is extremely important [47]. SOD catalyzes the dismutation of superoxide into hydrogen peroxide and water (Figure 1). There are three forms of SOD: SOD1 in the cytoplasm, SOD2 in the mitochondria, and extracellular SOD3. Cu/Zn SOD (SOD1) is found primarily in the cytoplasm and nucleus. Mn-SOD (SOD2) appears to be present only in the mitochondria, and extracellular SOD is in the extracellular space. Extracellular SOD activity is much higher in the vessel wall than other tissues, but Cu/ZnSOD and MnSOD constitute the majority of SOD activity [48].

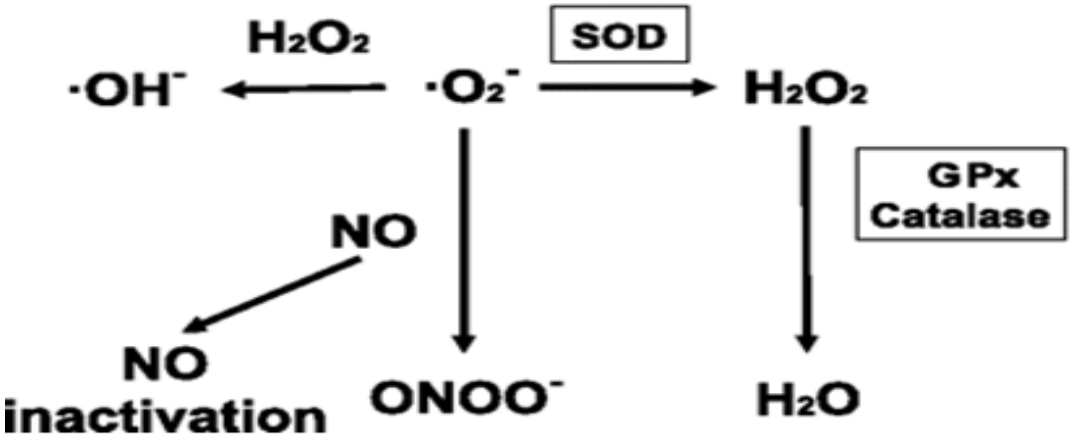

Figure 1: Degradation of superoxide and hydrogen peroxide from superoxide dismutase, catalase (CAT), and glutathione peroxidase (GPx). In this figure, superoxide is being degraded by either nitric oxide (NO) or superoxide dismutase (SOD). The SOD enzymes convert superoxide to hydrogen peroxide, which is then broken down by glutathione peroxidase and catalase to water. (·OH- (hydroxyl ion), ONOO- (peroxynitrate), NO- (nitric oxide), ·O2- (superoxide). Figure modified from [49].

Regulation and removal of hydrogen peroxide is important because it prevents the formation of the hydroxyl radical, which is highly reactive and damaging. The hydroxyl radical is formed by reacting hydrogen peroxide with Fe2+, known as the Fenton reaction [50]. The Fenton reaction plays a role in oxidative damage after oxidative stress conditions, which results in the accumulation of high levels of hydrogen peroxide and Fe2+ released from intracellular storage [51].

GPX and CAT are endogenous enzymes that reduce hydrogen peroxide into water. In mice, GPX-1 deficiency results in abnormal cardiovascular structure and function [52]. GPX-1 functions at low concentrations of hydrogen peroxide (5-8 μM) [53]. CAT is a heme protein located in peroxisomes, and also changes hydrogen peroxide into water. CAT uses hydrogen peroxide as a substrate and functions when hydrogen peroxide concentrations are above physiological levels (1-10 μM extracellular, 1-700 nM intracellular), which is common during oxidative bursts following stress responses [54]. While GPX is protective against lipid peroxides, CAT is not [55].

There are several ways to measure oxidative stress, which include assessing ROS levels, endogenous antioxidants, oxidative stress markers, and inflammation [56]. Measuring gene expression of enzymes like SOD, GPX, and CAT has been shown to predict oxidative stress levels in blood or tissue. For example, SOD activity is increased as ROS levels increase [57]. Lipids are also commonly used to measure oxidative stress because they are a target of ROS. Some measureable products of lipid peroxidation are malondialdehyde, short-chain alkanes, and lipid hydroperoxides. Proteins that have undergone oxidative stress become carbonylated, and measuring the amount of protein carbonylation can also indicate levels of oxidative stress. In our

current study, we use protein carbonylation, superoxide disumutase assays, and multiple measurements of antioxidant enzymes to measure the amount of oxidative stress.

Sirtuin Enzymes

Sirtuins are a class of deacetylase enzymes that are associated with mechanisms that enhance cellular homeostasis, aid in degenerative disease susceptibility, and are possibly involved with mediating redox stress [4]. The Sirtuin family of class III deacetylases, often referred to as SIR2 (silence information regulator 2), differs from the class I and class II deacetylases in that they are NAD+ dependent enzymes, while the other classes are zinc dependent [8]. Through NAD+ dependent deacetylation of proteins, sirtuins have been reported to increase lifespan through DNA repair and antioxidant mechanisms [8]. Currently, there are seven mammalian homologs in the SIR2 family: SIRT1-SIRT7 [58].

SIRT1

SIRT1 is a nuclear Sirtuin that has been shown to have an effect on lifespan and aging, and also plays a role in oxidative stress. SIRT1's impact on lifespan was first evident in yeast and worms, where an absence of the SIRT1 homologue led to a reduction in lifespan [59]. SIRT1 is also induced in response to low levels of oxidative

stress. Some regulatory events that occur during redox stress can modify the protein levels of SIRT1 [60], and there are a number of SIRT1 de-acetylation substrates that affect redox stress. P53, which is involved in activating antioxidant genes like SOD and GPX, binds to SIRT1. SIRT1 then de-acetylates p53, which weakens its transcriptional activity. The de-acetylation of p53 may serve to regulate the balance between antioxidant protection and apoptosis.

Another pathway that sirtuins can activate an antioxidant response involves the forkhead box O (FOXO) transcription factor family. SIRT1, SIRT2, and SIRT3 deacetylate and activate FOXO3a in response to oxidative stress [61, 62]. Activation of FOXO3a in response to oxidative stress is important because FOXO3a is a transcriptional activator of the antioxidant enzyme SOD2, and CAT. Low levels of hydrogen peroxide lead to the upregulation of FOXO3a-induced catalase, but higher levels lead to the switch to FOXO3a-mediated apoptosis [63].

Activation of SIRT1 confers cytoprotection in cardiomyocytes and has been shown to protect the heart from failure. In one study, an overexpression of SIRT1 by 2.5-7.5 fold decreased oxidative stress, cardiac hypertrophy, apoptosis, and cardiac dysfunction in response to oxidative stress and pressure overload in the hearts of transgenic mice [19]. The same study demonstrated an increase in oxidative stress, apoptosis, and cardiac hypertrophy where SIRT1 was increased by 12.5 fold, possibly because of mitochondrial dysfunction or NAD+ depletion. SIRT1 has also been shown to induce neonatal cardiomyocyte hypertrophy when overexpressed and activated by resveratrol [16]. It is evident that SIRT1 plays a role in cardiac oxidative stress, and

further studies are needed to better understand the exact role and mechanisms of this enzyme.

SIRT2

SIRT2 is a cytosolic enzyme that affects the regulation of redox stress [18]. Although SIRT2 is localized predominantly in the cytoplasm, it has been reported to be present in the nucleus during phases of mitosis. Redox stress causes an upregulation of SIRT2 that could be associated with apoptosis, but low levels of SIRT2 up-regulate mnSOD, causing a decrease in oxidative stress [18]. Hydrogen peroxide treatment in cells has shown to increase SIRT2 expression. SIRT2 binds to FOXO3a, increasing FOXO target genes including mnSOD, decreasing cellular levels of ROS [62]. SIRT2 has not been as widely researched as SIRT1 and SIRT3, but it is evident that SIRT2 plays a role in regulating redox stress. Further studies of SIRT2 relating to CVD pathologies is important to understand its role in cardiovascular redox stress.

SIRT3

SIRT3 is located in the mitochondria, and is involved in the synthesis and maintenance of cellular ATP levels in the heart, liver, and kidney [64]. Studies have shown that SIRT3 has the ability to suppress tumors, promote longevity in cells, and help decrease oxidative stress in the mitochondria [65]. SIRT3 was first shown to regulate SOD2 by modulating FOXO3a activity in the mitochondria, which led to subsequent FOXO3a-mediated SOD2 expression. FOXO transcription factors regulate many intracellular processes within the metabolism, and are also involved in cellular

resistance to various forms of oxidative stress [66]. A study using SIRT3 deficient mice demonstrated SIRT3 blocks the cardiac hypertrophic response in mouse hearts. SIRT3 deficient mice showed signs of cardiac hypertrophy and interstitial fibrosis at 8 weeks of age, and hypertrophic stimuli caused by angiotensin II to the mice produced a severe cardiac hypertrophic response. The wild-type mice seemed to have an augmented SIRT3 level, functioning as a protective response from the hypertrophic stimuli [66].

Niacin

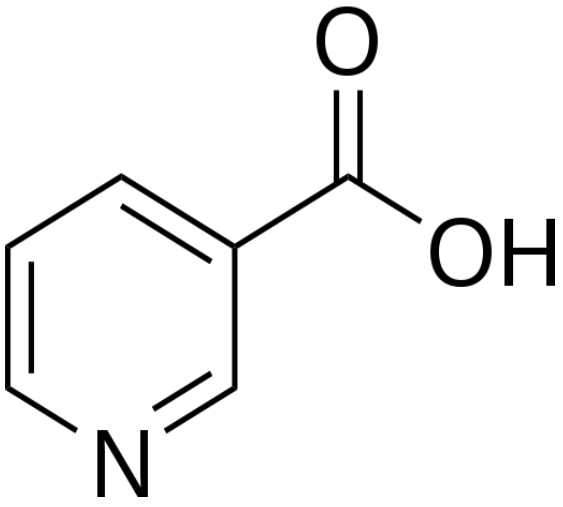

Figure 2: molecular structure of Niacin.

Niacin (vitamin B3) is one of the eight B vitamins (**Figure 2**) and is also called nicotinic acid. Niacin has a molecular formula of $C_6H_5NO_2$. There are two other forms of niacin, nicotinamide and inositol hexanicotinate, which have different biological

effects than niacin. Niacin binds to a G-coupled protein receptor called GPR109A. The binding of niacin stimulates the receptor and causes the inhibition of fat breakdown. The decrease in free fatty acids in the blood causes a decrease in the amount of very low-density lipoproteins (VLDL) from the liver. The reduction of VLDL, also known as "bad cholesterol," causes a decrease in blood pressure, and can cause an increase in high-density lipoproteins, the "good cholesterol," making it a common prescription for people with high blood pressure.

The effects of Niacin were first discovered during The Coronary Drug Project by Rudolph Altschul and Abram Hoffer [67]. The Coronary Drug Project was conducted between 1966 and 1975 to evaluate the long-term effects of niacin and four other lipid-influencing drugs. Participants in the study had previous myocardial infarction, ranged in age from 30-64 years, and had been free from myocardial infarction for at least three months. Niacin was administered in a 3000 mg/day dosage, and was the only drug seen to significantly reduce the risk of cardiovascular events during the six year period. Niacin was also the only drug to show significant lipid-lowering effects in this population. Compared to the placebo, the niacin group had a significantly lower incidence of non-fatal myocardial infarction (26%) and reduced cerebrovascular events (24%). Total cholesterol was reduced by 10% and triglycerides were reduced 26% in niacin-treated patients. In the 15 year follow up, mortality from all causes in the niacin group was reduced by 11% relative to the placebo group [67].

More than 50 years of extensive research has proven that niacin is an effective treatment for dyslipidemia, atherosclerosis, high-blood pressure, and other health issues. Recent discoveries provide additional insight into the potential vascular anti-

inflammatory and anti-oxidative properties of niacin, which may aid in reducing atherosclerosis [3]. Niacin is a precursor for the synthesis of nicotinamide adenine dinucleotide (NAD+), and has been shown to increase cellular concentrations of NAD+. Precursors of NAD+ have been shown to upregulate the expression of glucose-6-phosphate dehydrogenase, which in turn, increases nicotinamide adenine dinucleotide phosphate (NADPH). An increase in NADPH levels can cause a decrease in cellular ROS. In a study using human aortic endothelial cells, niacin increased NADPH and reduced glutathione peroxidase levels and LDL oxidation [68]. In a study where diabetic patients were treated with Niacin for three months (1500 mg/day), the niacin treated patients had increased HDL plasma levels, increased HDL capacity to stimulate endothelial NO production, increased endothelium-dependent vasodilation, and reduced lipid peroxidation [68]. Additional study of the effects of niacin on oxidative stress in the heart could potentially provide more insight on exactly how niacin functions to decrease cardiovascular risks.

Obesity and Oxidative Stress in CVD

There is an extensive amount of data linking oxidative stress and ROS to the pathophysiology of CVD. Oxidative stress is evident in all facets of heart failure, including genetic abnormality, pressure overload from hypertension, and infarction [71]. A variety of enzymatic and non-enzymatic processes can generate ROS in mammalian

cells, including the mitochondrial respiratory chain, NADPH oxidases, xanthine oxidase, and lipoxygenase, and there is evidence linking each of these sources with CVD pathology.

ROS participate in cell signaling in the vascular walls, and are produced in all vascular cell types including endothelium, smooth muscle, and adventitia [69]. ROS act as signaling molecules under low concentrations, regulating vascular smooth muscle contraction, relaxation, and growth [70], [42]. Some physiologic stimuli that have been shown to contribute to CVD also activate the formation of ROS. For example, Angiotensin II is a vasoactive agent that also increases NADPH oxidase expression [71]. Vascular NADPH oxidase can also be regulated by growth factors, cytokines, and hemodynamic forces [72], [73]. Animal experiments have shown NOX isoforms to play a role in other types of CVD like cardiac fibrosis [74], ischemic preconditioning [75], and cardiac remodeling post myocardial ischemia [76].

In the mitochondria, superoxide is generated in high amounts, which is dismutated to hydrogen peroxide by Mn-SOD [77]. Mutant mice that lacked the Mn-SOD gene died within the first 10 days of life due to dilated cardiomyopathy. There was a significant decrease in succinate dehydrogenase (complex II) and aconitase (TCA cycle) activities in the heart and other organs [78]. Another study used heart/muscle-specific manganese superoxide dismutase-deficient mice to study the effects of oxidative stress in heart failure. The mutant mice developed progressive congestive heart failure with specific molecular defects in mitochondrial respiration [79]. This data shows the mitochondria is an important source of ROS and the inability of antioxidants to regulate the ROS can lead to cardiac dysfunction.

Oxidative Stress and Obesity

Obesity is a condition in which excess body fat has accumulated to an extent that it may cause an adverse effect on health. Obesity can ultimately lead to reduced life expectancy and/or increased health problems [55]. Oxidative stress has been linked to obesity, adiposity, insulin resistance, and metabolic syndrome [80]. Studies have shown a positive correlation between increased body mass index (BMI) and waist/hip ratio and increased oxidative stress [81]. Even children with obesity and no other symptoms of metabolic syndrome have increased levels of oxidative stress and endothelial dysfunction [64]. Obesity causes hyperglycemia, increased tissue lipid levels, inadequate antioxidant defenses, increased rates of free radical formation, and chronic inflammation, which are all sources of increased oxidative stress. Chronic hypernutrition, high fat high carbohydrate meals, as well as high dietary saturated fatty acids and trans-fatty acids, stimulate intracellular pathways, leading to oxidative stress through multiple biochemical mechanisms. These mechanisms include superoxide generation from NADPH oxidases (NOX), oxidative phosphorylation, glyceraldehyde autoxidation, protein kinase C (PKC) activation, and polyol and hexosamine pathways [6].

Obesity related oxidative stress in CVD

Cardiac lipid accumulation from obesity is a major risk factor for CVD [82], and one of the well-known targets for oxidative injury is lipid peroxidation. Lipid peroxidation produces hydroperoxides, which have toxic effects on cells, and can react with transition metals like iron or copper to form stable aldehydes such as dialdehydes that have the potential to damage cell membranes [83]. Lipid peroxides also inhibit the synthesis of prostacyclin, which leads to increased platelet aggregation and potentially thrombosis [84].

In 2011, albino rats were used to study the effect of high-fat diet on oxidative stress in the liver, kidney, and heart [55]. The rats were placed on a sixteen week high-fat diet, and showed an increase in oxidative stress markers and a decrease in antioxidant genes in the liver, heart, and kidney. The high-fat diet group was fed a 46% fat diet and the control group was fed a 5% fat diet. In the mouse heart tissue, there was a significantly increased level of malondialdehyde and protein carbonyl in the obese group compared to control. There was also a significant decrease in the antioxidant enzymes glutathione S- transferase, GPx-1, and paraoxonase1 [55]. The liver and kidney also showed signs of oxidative stress in the obese rats.

A study in 2011 examined the effect of weight loss on preservation of heart function and attenuation of left ventricular remodeling, oxidative stress and inflammation in obese mice [85]. Eight-week-old C57BL/6J mice (n=24) were equally divided into

control, obesity, and obese reduction for 22 weeks. The obese reduction group was fed a high-fat diet for fourteen weeks, and then fed the control diet for the remaining eight weeks. The heart weight, body weight, abdominal-fat weight, total cholesterol level and fasting blood glucose were higher in obesity than in control and in the obese reduction groups. Protein and mRNA expressions of NOX1 and NOX2, HO1 and NQO1 were higher in the obese group compared to control and obese reduction. Adiponectin mRNA expression was decreased in the obese group compared to control and obese reduction. When comparing only the obese group to control, the obese group had a significant increase in NOX1, NOX2, HO1 and NQO1. The obese group also had a significantly larger heart weight than the control group, indicating that the 14 week diet did induce oxidative stress and early signs of heart failure. This study suggests that oxidative stress induced from a high-fat diet can be reversed with weight loss.

CVD is the most common cause of mortality and morbidity in people with type I and type II diabetes [86]. However, the exact mechanism that accelerates the prevalence of CVD is not completely understood. Some factors that have been associated with increased CVD in diabetics include poor glycemic control, markers of insulin resistance, low-grade inflammation, and oxidative stress [46]. NADPH oxidases have been shown to facilitate the progression of diabetic cardiomyopathy. The inhibition of NADPH oxidase by an NADPH oxidase activity inhibitor called apocynin, has been shown to decrease instances of diabetes-induced myocardial contractile dysfunction in mice [87].

Adiponectin

In addition to energy storage, adipose tissue functions as an endocrine organ by secreting numerous molecules that can affect metabolism. Adiponectin is one of the most abundant hormones secreted from adipose tissue. Adiponectin was initially discovered in 1995 [88], but until 2001, its relevance remained largely unknown. In the years since, adiponectin has been found to play distinct roles in the balance of energy homoeostasis. Previous research demonstrated the potential anti-diabetic, anti-atherosclerotic and anti-inflammatory properties of adiponectin, leading to numerous clinical studies on the relevance of adiponectin and metabolic disease [89].

Adiponectin in its most basic form is a 30kDa subunit homotrimer. Adiponectin undergoes post translational modifications to form high order structures including low-molecular weight hexamers (180 kDa) and high-molecular weight 16–18mers (greater than 400 kDa) [89]. Adiponectin concentrations are normally between 2 and 20 mg/mL, which can be up to 0.05% of total serum protein [88]. Circulating levels of adiponectin are lower in people with obesity compared to lean individuals, and women have higher circulating levels of adiponectin than men. Adiponectin levels are also reduced in people with cardiovascular disease [90] and diabetes [91]. Increased plasma adiponectin levels significantly increase insulin sensitivity independent of variables such as obesity and gender [92]. Triglycerides are also negatively correlated with plasma adiponectin.

Regulation of Adiponectin Production and Secretion

Adiponectin is regulated transcriptionally and post-transcriptionally. Some key factors that regulate adiponectin production and secretion are peroxisome proliferator-activated receptor γ (PPARγ), tumor necrosis factor alpha (TNFα), interleukins, CCAAT-enhancer-binding proteins C/EBPα, and a disulfide-bond A oxidoreductase-like protein DsbA-L. PPARγ is a nuclear receptor and transcription factor. It is expressed in adipose tissue, and is a positive regulator for adiponectin gene expression, production, and secretion [93]. When activated, PPAR-γ increases adiponectin gene expression, production and secretion [94]. Deletion of PPARγ in adipose tissue of mice results in adipocyte hypocellularity and hypertrophy and decreased levels of adiponectin [95]. Under nutrient restriction, SIRT1 inhibits PPAR-γ by binding to genes that regulate PPAR-γ expression, causing the mobilization of fatty acids. In SIRT1+/− mice, mobilization of fatty acids from adipocytes is compromised [15]. PPARγ agonists, like Thiazolidinediones (TZDs), have been shown to increase insulin sensitivity, circulating adiponectin, and adiponectin concentrations in adipose tissue [93]. The transcription factor C/EBPα has also been shown to stimulate the production of adiponectin. TNF-α and IL-6 have a negative association with adiponectin and their expression and secretion of TNF-α and IL-6 increases in the adipose tissue of obese subjects. Disulfide-bond A oxidoreductase-like protein (DsbA-L) is protein that interacts with adiponectin. DsbA-L facilitates adiponectin folding and assembly and provides a

protective effect against ER stress-mediated adiponectin down-regulation in obesity [96].

Physiological Effects of Adiponectin

Adiponectin exerts multiple biological effects throughout the body and is mediated by the receptors AdipoR1, AdipoR1, and T-cadherin [97]. AdipoR1 and AdipoR1 serve as receptors for globular and full length adiponectin, and mediate fatty acid oxidation and glucose uptake by adiponectin. AdipoR1 exhibits high affinity binding and AdipoR2 exhibits intermediate binding affinity. AdipoR1 is mainly expressed in skeletal muscle, while AdipoR1 is mainly in the liver [98]. The expression of the receptors AdipoR1 and AdipoR1 have been shown to decline by thirty percent in the subcutaneous fat of obese individuals, but normalize when weight loss is accomplished [99]. In streptozotocin (STZ) induced diabetic rat hearts, adiponectin receptors were upregulated in the heart and skeletal muscle. Although the receptors were upregulated, circulating adiponectin was decreased. Normal AdipoR1 levels were restored by insulin administration [100, 101].

T-cadherin is a glycosyl phosphatidylinositol-anchored cell surface glycoprotein that is ubiquitously expressed. The highest expression of T-cadherin is found in the heart and the aortic, carotid, iliac, and kidney arteries [97]. T-cadherin has been shown to protect against cardiac stress in mice through its association with adiponectin. T-cadherin deletion in mice eradicated adiponectin cardioprotective effects in cardiac hypertrophy and myocardial ischemia-reperfusion injury [102].

Clinical studies have identified a negative correlation between adiponectin and various aspects of CVD including atherosclerosis, myocardial infarction, heart failure, endothelial dysfunction and hypertension [103]. High-molecular weight adiponectin was previously thought to be the main predictor of CVD, but recent research shows that the low-molecular weight adiponectin might be a potential biomarker for CVD [104]. The beneficial effect of adiponectin on CVD comes from its ability to induce anti-oxidative, metabolic, anti-fibrotic, anti-apoptotic, and anti-inflammatory effects. The hearts of mice lacking adiponectin have an exaggerated response to cardiac stress. This response was alleviated after restoration of circulating adiponectin [103]. Adiponectin has also been shown to lower oxidative stress in the heart. Treatments of exogenous adiponectin reduced ROS production and apoptosis in cardiac H9C2 cells that were subjected to hypoxia and reperfusion [105].

Most data relating adiponectin and CVD indicate the beneficial effects of adiponectin, but some studies suggest that adiponectin can have a negative effect on the cardiovascular system. For example, one study found that high levels of adiponectin correlate with mortality and severity in patients with congestive heart failure [106]. Adiponectin knockout mice subject to chronic stress from long term pressure overload had preserved oxidative capacity and cardiac function compared to the wild-type mice [107]. This data suggests that that adiponectin may be playing a permissive role in long-term cardiac dysfunction.

For many years adiponectin was thought to be exclusively secreted by adipose tissue, but recent research has found adiponectin to be expressed in cardiomyocytes and epicardial adipose tissue [108, 109]. Cardiomyocyte-derived adiponectin directly

regulates cardiac metabolism by AMPK activation via cardiac AdipoR1 and AdipoR2 [110]. The exact mechanisms of cardiac adiponectin are still unknown, and there is an ongoing debate as to whether adiponectin is actually produced in the heart. It is important to further research these questions in order to gain a better understanding of the effects of adiponectin on diseases related to the heart and cardiovascular system.

Materials and Methods

1- Effect of a high fat diet on oxidative stress in the mouse heart

1.1 – Mouse Study Design:

Tissues for this study were collected from mice that were initially part of a separate study. The study was designed to examine the effects of niacin treatment on adiponectin levels in mice fed a high fat diet. We decided to examine whether this treatment had any effect on oxidative stress in the heart. 57BL/6 mice (n=32) were used for this study. Mice were weighed and randomly separated into two groups (n=16). Mice were fed a control (10% kcal as fat) or high fat (60% kcal as fat) diet for 6 weeks. After 6 weeks on diets, mice on control and high fat diet were started on vehicle (n=8) or .3% niacin (n=8) in water and were treated for 5 additional weeks. The mice were on the diet for a total of 11 weeks. At the end of the treatment periods, mice were decapitated and the hearts and kidneys frozen in liquid nitrogen and stored at -80° C.

1.2- RNA isolation from mice:

1.2.1 - Isolation of total RNA: Hearts and kidney were removed from the -80° C freezer, fractured in liquid nitrogen and approximately 20-30 mg used for RNA isolation. The tissue was homogenized in 1 mL of Trizol (Invitrogen, 1mL trizol/100mg tissue) using a polytronix tissue homogenizer (Fisher Scientific, Pittsburg, PA) for thirty

seconds. Samples were centrifuged at10,000 x g for fifteen minutes at 4˚C. After centrifugation, chloroform (200 uL/ mL Trizol) was added to the supernatant of each sample, shaken, allowed to incubate at temperature for three minutes and then centrifuged at 10,000 x g for fifteen minutes at 4˚C. The samples separated into three layers after centrifugation. A bottom organic layer, a white middle layer, and an aqueous top layer that contains total RNA. This layer was carefully removed and transferred to a new 1.5 mL eppendorf tubes. Total RNA was then isolated from the aqueous phase using the RNeasy Plus Mini Kit (Qiagen Inc., Valencia CA). The aqueous layer was transferred to a DNA eliminator column and centrifuged at 10,000 x g for fifteen seconds at room temperature to remove genomic DNA. The flow through was saved and 700 microliters of 70% ethanol in diethyl pyrocarbonate (DEPC) water was added and mixed by pipetting. Samples were transferred to an RNA spin column and centrifuged at 10,000 x g for thirty seconds. The flow-through was discarded and column was saved. Samples were then washed with 700 microliters of wash buffer and centrifuged for thirty seconds. Then samples were washed twice with 500 microliters of RPE buffer and centrifuged first for thirty seconds, and the second time for two minutes. The old collection tube was discarded and the column was centrifuged with a new 2 mL tube for one minute. The collection tube was discarded and replaced with a new pre-labeled 1.5 milliliter collection tube for. Nuclease-free water (30ul) was added to the column and centrifuged for one minute to extract the RNA. The RNA was either stored at -80˚C or used in the following steps.

1.2.2 - RNA purity concentration analysis**:** The samples of RNA were analyzed spectophotometrically for concentration and purity. The absorbance was determined by

UV spectroscopy using a SmartSpec plus spectrophotometer (Bio-Rad, Hercules, CA). RNA was diluted 1:10 in 1X TE buffer, and transferred to a 50 microliter cuvette, using 1X TE buffer as the blank. An absorbance at 260 nm of one is equal to 40 micrograms/mL of total RNA. The concentration of tissue RNA ranged from 0.42-0.89 micrograms RNA/mg tissue. The 260/280 ratio that was greater than 1.7 was used for cDNA synthesis.

1.3 - Real-Time PCR primer design:

PCR primers were designed using the PCR primer design tool at operon.com. Guidelines for primer design were a 18-24 base pair length, GC content of 50-60%, and a melting temperature between 50-65° C. Full length genes were first analyzed for secondary structures using Mfold (http://mfold.rna.albany.edu/?q=mfold/dna-folding-form). Mfold condition were; folding temperature, 60° C, ionic sodium conditions 50 millimoles/L, magnesium 3 millimoles/L. Sequences of 75-150 base pairs that had no secondary structures were used for primer design. Gene specific primers were designed for Superoxide dismutase 1 (SOD-1), Superoxide dismuate 2 (SOD-2), Glutathione peroxidase-1 (GPx-1), ribosomal protein 36B4, NADPH Oxidase-1 (NOX1), NADPH Oxidase-2 (NOX2), NADPH Oxidase-4 (NOX4), P47phox, p67phox, Catalase, Glyceraldehyde-3-phosphate dehydrogenase (GAPDH), beta-actin, adiponectin, and mitochondrial cytochrome-b (mt-cyb).

1.3.1- Primer Design Confirmation: In all situations, primer design for each gene was confirmed by either product size verification using electrophoresis on agarose gel or by

sequencing PCR products following cloning. To determine PCR product sizes, PCR products were added to gel loading buffer dye and electrophoresed on a 2% agarose gel in 1XTAE buffer. DNA standards (50-1000 bp) were used for size estimations. Gels were stained with ethidium bromide (1ug/ml) for 3 min and then destained in H20. Wells were visualized under UV light and photogragraphed using a BioRad FlourS imager. Each PCR product size was then compared to the calculated product size based on PCR primers. Criteria for inclusion of a primer pair for further use was the occurrence of only one band at the theoretical size.

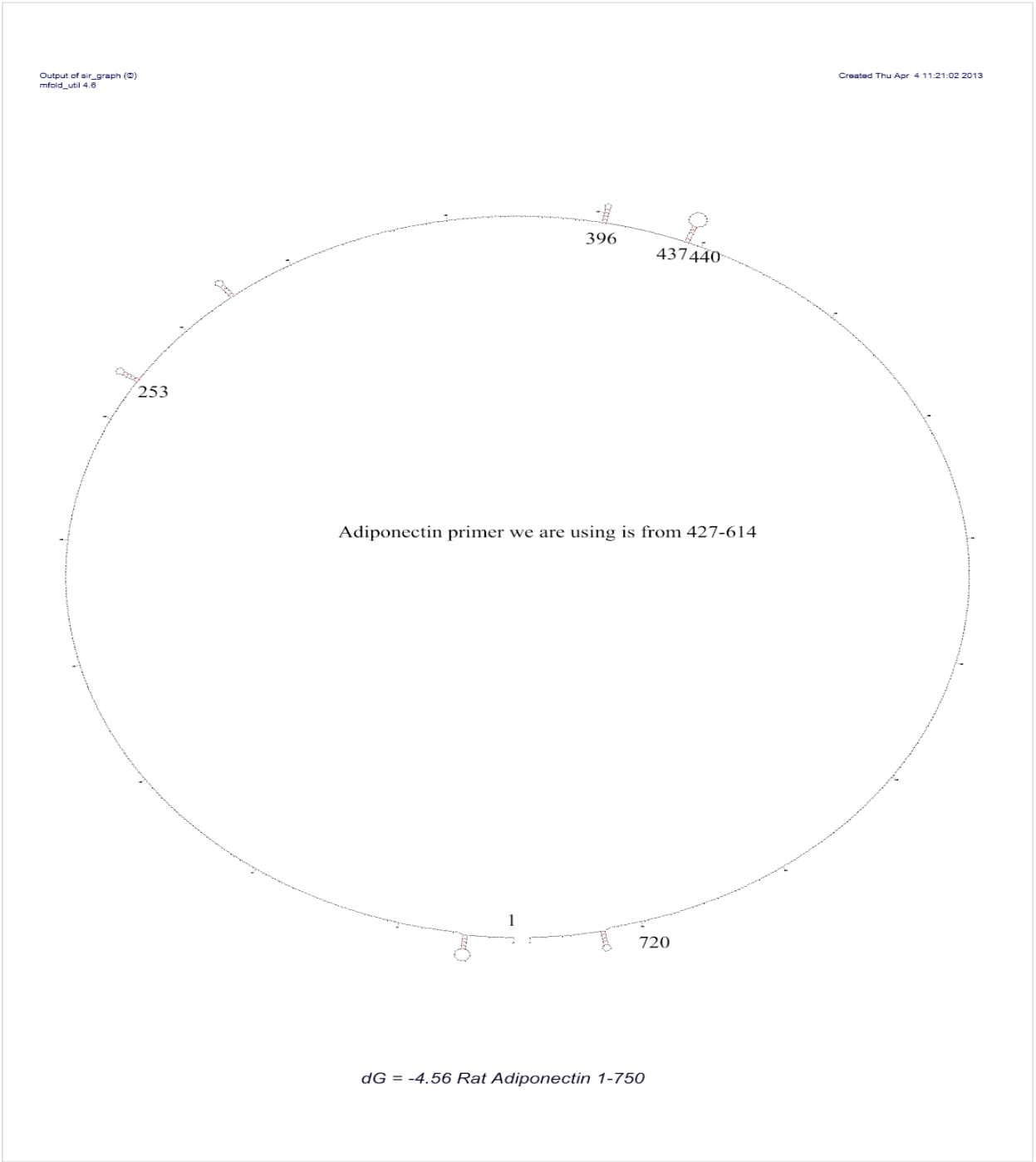

Figure 3: This figure depicts the adiponectin amplicon folded at 60°C with 50 mM Na+ and 3mM Mg 2+. CDS sequence was found on gene bank and analyzed for secondary structures using Mfold (http://mfold.rna.albany.edu/?q=mfold/dna-folding-form_. Sequences of 75-150 base pairs that had no secondary structures were used for primer design. Primers were created in the 427-614 region.

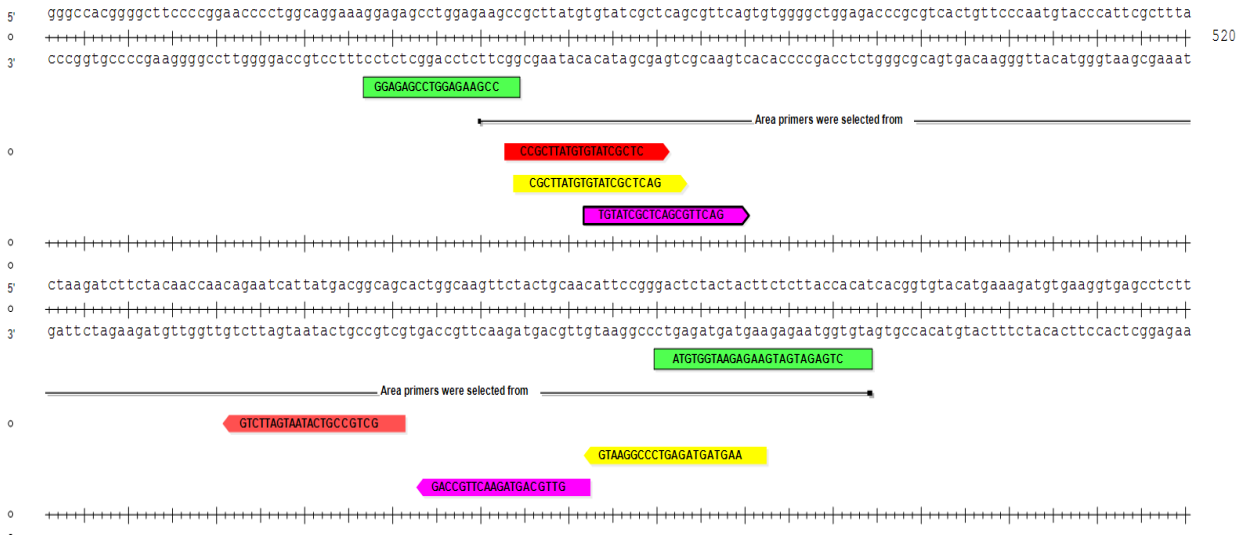

Figure 4: This figure represents the CDS region of the adiponectin gene from a BLAST search on gene bank for gene specifity. BLAST is a search of all genes stored in the NCBI GenBank database and is available online at www.ncbi.nih.gov/Genbank. The highlighted areas are the forward and reverse sequence of the four adiponectin primers that were created. Criteria for primer selection included folding temperature, 60° C, ionic sodium conditions 50 millimoles/L, magnesium 3 millimoles/L. Sequences of 75-150 base pairs that had no secondary structures were used for primer design. Primers were created in the 427-614 sequence of the CDS region. Dr. Desiree Wanders created the green primer sequence.

1.4 - Cloning PCR Gene Products:

The gene-specific primers superoxide disumatase-1, superoxide dismutase-2, glutathione peroxidase-1, and 36B4 that were created were cloned for sequencing standard curve generation. Cloning was carried out using the StrataClone PCR cloning kit. The ligation mixture was prepared using 3 uL of StrataClone Cloning Buffer, 2uL of the PCR product, and 1 uL StrataClone Vector Mix amp/kan. The mixture was incubated at room temperature for five minutes and 1 uL of the mixture was added to a tube of competent cells from the StrataClone solo pack. The mixture was incubated for 20 minutes on ice, then heat shocked at 42° C for 45 seconds. The mixture was then put on ice for 2 minutes. 250uL of pre-warmed LB medium was added to the mixture. The mixture was incubated at 37° C with agitation for one hour. During this time, LB-ampicillin plates for blue white screening were prepared by spreading 40 uL of 2% X-gal on each plate. X-gal is a galactose sugar that is metabolized by B-galactoside to form an insoluble product that appears blue. This is a negative indicator. White colonies indicate insertion of target DNA meaning the cell no longer has the ability to hydrolyze X-gal. Since normal bacterial colonies would also appear white, the plates had ampicillin, an antibiotic in the growth medium and a resistance in the gene on the vector to allow a successful transformation of bacteria to survive. After the hour agitation and incubation, the transformation mixture was plated onto the LB-ampicillin plates. Amounts of 5 uL for one plate and 100 uL for a second plate for each gene were spread

on each plate. These plates were incubated at 37° C overnight. The next day five white or light blue colonies were picked for plasmid DNA analysis. These colonies were grown overnight at 37° C in LB medium.

1.6 - Plasmid isolation:

Plasmids were isolated using a Zyppy Plasmid Miniprep kit (Zymoresearch) according to manufacturer's instructions. Briefly, 600 µl of bacterial culture grown in LB centrifuged at 11,000 x g and the supernatant discarded. 600 µl of 1XTE was added to the bacterial cell pellet and resuspend completely. Bacterial cells were lysed in Lysis Buffer, then 350 µl of cold Neutralization Buffer was added and mixed thoroughly. Samples were centrifuged at 11,000 – 16,000 x g for 2-4 minutes and the supernatant was transferred into a Zymo-spin column and centrifuged for 15 seconds. The flow through was discarded. Then 200 µl of Endo-Wash Buffer was added to the column and the samples were centrifuged for 30 seconds. 400 µl of Wash Buffer was added to the column and centrifuged again for 1 minute. The column was transferred into a clean 1.5 ml microcentrifuge tube and 30 µl of Elution Buffer 2 was added directly to the column matrix and allowed to stand for one minute at room temperature. The column was centrifuged for 30 seconds to elute the plasmid DNA

1.6.1 - Plasmid DNA Concentration and analysis: Plasmid concentrations were measured spectrophotometrically using a SmartSpec plus spectrophotometer (Bio-Rad, Hercules, CA). Plasmid DNA was diluted 1:10 in 1X TE buffer, and transferred to a 50 microliter cuvette, using 1X TE buffer as the blank. An absorbance at 260 nm of one is equal to 50 micrograms/mL of total RNA.

The adiponectin plasmid was sent for sequence analysis at Eurofins MWG Operon, Hunstville Al. T7 primers were used for the sequence analysis because they are the primers specific for the Strata Clone pSC-A-amp vector used in section 1.4. Following sequence analysis, the sequences were BLAST search for gene specificity. BLAST is a search of all genes stored in the NCBI GenBank database and is available online at www.ncbi.nih.gov/Genbank.

Next, primer PCR efficiency was determined by real-time PCR using a myIQ iCycler real-time PCR detection system (Bio-Rad). A standard curve was generated using 10-fold dilutions of plasmid. The reaction mixture was as follows 12.5 microliters of SYBR green super mix, 6.5 microliters of nuclease-free H20, 1 microliter of primer mix of 20uM concentration (both sense and antisense mixed in 1XTE buffer) and 5 microliters of plasmid. The thermocycler program was as follows: an initial denaturation at 95° C for 10 min, followed by 40 cycles of 95° C for 15 seconds, 58° C for 30 seconds and 55° C for 1 minute, then 1 minute at 72° C. Only primers with efficiencies of 90-120% were used for experiments.

1.5 - Evaluation of mRNA expression:

1.5.1 - First strand cDNA synthesis: First strand cDNA was synthesized using the iScript First Strand Synthesis kit (BioRad). One microgram of total RNA was used for each sample, along with one microliter of reverse transcriptase, and four microliters of reaction mix, for a final volume of 20 microliters. The reaction was carried out on a

BioRad MyIG thermocycler. The conditions were 25° C for five minutes, followed by 42° C for thirty minutes, then 85° C for five minutes with an infinite hold at 4° C.

1.5-2 - Real-Time PCR: Real-time RT-PCR analysis was performed on control and high fat diet mouse hearts, and in some cases kidneys. The reaction mixture was as follows: 12.5 microliters of SYBR green super mix, 10.5 microliters of nuclease-free H20, 1 microliter of primer mix of 20uM concentration (both sense and antisense mixed in 1XTE buffer) and 1 microliter experimental cDNA. Each sample was run in duplicate. The thermocycler program was as follows: an initial denaturation at 95° C for 10 min, followed by 40 cycles of 95° C for 15 seconds, 58° C for 30 seconds and 55° C for 1 minute, then 1 minute at 72° C followed by a melt curve of 80 cycles starting at 55°C and increasing 0.5°C each cycle. A melt curve was performed to ensure there was no primer dimerization.

1.5-3 Real-time PCR analysis: Changes in gene expression calculated relative to the gene expression of the control diet set at 1 fold change. Calculations are derived from the algorithms outlined by Vandesompele et al [111] and was programmed into Bio-Rad Gene Expression Macro excel workbook and used for the analysis of gene expression.

Table 1: Gene Specific Primers for PCR

SOD-1 Accession # NM_011434	Sense 5' –CATCAGTATGGGGACAATACAC Antisense 5' -CCAACATGCCTCTCTTCATC
B-actin Accession # NM_007393	Sense 5' –CTGCCTGACGGCCAGG Antisense 5' -GGAAAAGAGCCTCAGGGCAT
MT-cytB Accession # JX457724	Sense 5' -CCACTTCATCTTACATTTCTTATCGC Antisense 5' -TTTTATCTGCATCAGTTTAATCCTGT
SOD-2 Accession # NM_013671	Sense 5' –TAAGGAGAAGCTGACAGCCGTG Antisense 5' -AATCCCCAGCAGCGGAATAAG
GPx-1 Accession # NM_008160	Sense 5' -CCAGGAGAATGGCAAGAATG Antisense 5' -CTTCGCACTTCTCAAACAATG
KIM-1 Accession # NM_134248	Sense 5' – ATGAATCAGATTCAAGTTC Antisense 5' - TCTGGTTTGTGAGTCCATGTG
36B4 Accession # NM_007475	Sense 5' –CACTGCTGAACATGCTGAAC Antisense 5' -CCACAGACAATGCCAGGAC
NOX1 Accession # NM_172203	Sense 5' –AGAAAGCCATTGGATCACAAC Antisense 5' -GGAGAGAACAGAAGCGAGAG
NOX2 Accession #FJ168469	Sense 5' –AAACTGGACAGGAACCTCAC Antisense 5' -GCATTCACACACCACTCAAC
NOX4 Accession #NM_015760	Sense 5' –GCAGCCTCATCCTTTTACC Antisense 5' -ACATGCACACCTGAGAAAATAC
P22phox Accession #Eu791539	Sense 5' –ACTGCTGGACGTTTCACAC Antisense 5' -CCCTTTTTCCTCTTTCCCCG
P47phox Accession #AB002663	Sense 5' –CATGTTCCTGTTAAGTGGC Antisense 5' -TGGGATGACTCTGTTCTCTG
P67phox Accession #AB002664	Sense 5' –ACCTCVCTAATTCTAGCCCCC Antisense 5' -TCCATGACCACTGTGTATTTG
CAT Accession #NM_009804	Sense 5' –AGCCAGAAGAGAAACCCAC Antisense 5' -ACAAGAAAGAAACCTGATGGAC
SIRT1	Sense 5' – CCAGATCCTCAAGCCATGT

Accession # NM_019812	Antisense 5’ - TTGGATTCCTGCAACCT
SIRT2 Accession # NM_022432.4	Sense 5’ – TACCCAGAGGCCATCTTTGA Antisense 5’ - TGATGTGTGAAGGTGCCGT
SIRT5 Accession # NM_178848	Sense 5’ – AGCAAGATCTGCCTCACCAT Antisense 5’ - GGATTTCCAGCAGCTTCTTG
SIRT7 Accession # NM_153056.2	Sense 5’ – TCTCTGAGCTCCATGGGAAT Antisense 5’ - CATGAGGAGCCCGCATTACAT
ADIPOQ Accession #BC028770	Sense 5’ – GGAGAGCCTGGAAGCC Antisense 5’ - ATGTGGTAAGAGAAGTAGTAGAGTC
GAPDH Accession #NM_008084	Sense 5’ –ATGAATCAGATTCC Antisense 5’ -CACATTGGGGGTAGGACCAC
PgK1 Accession #NM_008828	Sense 5’ –CAAGGTTTGGAGAGTCCAG Antisense 5’ -CAGCTGGATCTTGTCTGCAA

1.7 - Western Blot

Heart tissue samples were homogenized in RIPA (Radio-Immunoprecipitation Assay) buffer from Thermo Scientific, Rockford, IL containing 0.1% of halt protease and phosphatase inhibitor 100x (Thermo Scientific, Rockford IL) and 0.1% of PMSF. Samples were standardized to 5 mg/mL of protein and boiled in an equal amount of Laemmle buffer containing 5% β-mercaptoethanol. Samples were separated on a 4-20 or 10% polyacrylamide gel electrophoresis (SDS-PAGE) and then transferred to nitrocellulose membrane. Ponceau stain was added to the membrane to visualize the proteins to ensure transfer was successful. Membrane was then soaked in PBS to remove the ponceau stain. Membrane was blocked at room temperature with 4 mL Odyssey blocking buffer (LICOR Lincoln, NE) with equal amount of PBS for one hour. The membrane was then incubated with 6-7 mL IgG primary antibody at indicated dilutions overnight at 4° C. The membrane was washed four times for five minutes each with 10 mL of PBS with 0.1% tween 20 then incubated with IgG secondary antibody at an infrared intensity of 680 or 800 at room temperature for one hour. The membrane was washed again four times five minutes each with 10mL of PBS with 0.1% tween20. A Licor Odyssey imager was used to detect the immunoreactive bands. Each western blot was repeated twice. Blots were analyzed using the Odyssey Software v2.0. Beta-actin (Mouse anti-Actin, Millipore, Billerica, MA, MAB1501; 1:1000) was run as a loading control protein, and protein levels were standardized by dividing intensity by beta-actin intensity. Antibodies that were used for the experiments are in table 2.

1.7-2 Determining Protein Concentrations for Western Blot: Protein concentration was determined using the DC protein assay (Bio-Rad). A standard curve was generated using bovine serum albumin (BSA) diluted in lysis buffer at concentrations ranging from 0.25 to 1.5 micrograms/microliter. The absorbance was measured at 750 nanometers on a SpectraMax Plus microplate reader (Molecular Devices, Palo Alto, CA). Sample protein concentrations were determined based on the generated standard curve.

Table 2: Primary and secondary antibodies used for western blot.

1° IgG polyclonal Ab name	**Host**	**Supplier**	**Product Number**	**Dilution**
anti-actin	Mouse	Millipore, Billerica, MA	MAB1501R	1:500
anti-sirt1	rabbit	Millipore, Billerica, MA	09-844	1:500
Adiponectin	rabbit	Abcam, Cambridge, MA	ab3455	1:500
2° Ab name	**IRDye**	**Supplier**	**Product Number**	**Dilution**
2° Goat Anti-mouse IgG	800 CW	LICOR Odyssey Lincoln, NE	926-32210	1:14000
2° Donkey anti-goat IgG	800 CW	LICOR Odyssey Lincoln, NE	926-32214	1:14000
2 Goat anti-rabbit IgG	680 RD	LICOR Odyssey Lincoln, NE	926-32221	1:14000
2° Goat Anti Rabbit IgG	800 CW	LICOR Odyssey Lincoln, NE	926-32211	1:14000

1.8 - Evaluation of Protein Carbonyl Content:

Protein carbonyl content was measured in the mouse hearts as an indicator of oxidative stress (Cayman's Protein Carbonyl Colorimetric Assay Kit). The kit utilizes the dinitrophenylhydrazine (DNPH) reaction to measure the protein carbonyl content in tissue homogenates. 15-150 mg of tissue was homogenized in 0.8 milliliters to 1.5 milliliters of 50mM Phosphate buffer, pH 6.7, containing 1mM EDTA. The tissue was then centrifuged at 10,000 x g for 15 minutes at 4° C. The supernatant was removed and the supernatant not being used that day was stored in a -80° C freezer. To make sure there was no contaminating nucleic acids present in the sample, the absorbance was checked at 280 nm to assure that the 280/260 ratio was greater than one. 200 microliters each of the homogenized tissue samples were put in two 2 milliliter plastic tubes. DNPH (800 uL) was added to one tube, and 2.5 M HCL (800 uL) was added to the other tube. The tubes were incubated at room temperature for an hour, vortexed briefly every 15 minutes. Trichloroacetic acid (TCA) (1 mL of a 20% solution) was added to each tube, vortexed, and tube swere placed on ice for 5 minutes. The tubes were centrifuged for 10 minutes at 10,000 x g at 4° C, the supernatant was discarded and pellets were resuspended in 1 mL of 10% TCA and set on ice for 5 minutes. The tubes were centrifuged for 10 minutes at 10,000 x g at 4° C. The supernatant was then discarded and the pellets were resuspended in 1:1 Ethanol/Ethyl Acetate manually with a spatula, vortexed thoroughly, and then centrifuged for 10 minutes at 10,000 x g at 4° C. This

step was repeated two more times. After the final wash, the pellets were resuspended in guanidine hydrochloride (500 uL) by vortexing and centrifuged for 10 minutes at 10,000 x g at 4° C to remove any leftover debris. 220 microliters of the supernatant of all the control and sample tubes were transferred to a 96-well plate and measured at 370 nm using a SpectraMax Plus microplate reader (Molecular Devices, Palo Alto, CA). Protein carbonyl content was measured by the following equation. 0.011 µM is the adjusted extinction coefficient for DNPH.

Protein Carbonyl (nmol/ml) = [(CA)/(*0.011 µM-1)](500 µl/200 µl).

1.8.1 - Determination of protein concentration: To determine the protein carbonyl content, the protein concentration of the samples was determined. The absorbance of the control supernatants were determined using a SmartSpec plus spectrophotometer (Bio-Rad, Hercules, CA). A bovine serum albumin (BSA) standard curve was generated (0.15-2.0 mg/ml) dissolved in guanidine hydrochloride. 100 microliters of the samples, and standard curve samples were placed in a 1 mL quartz cuvette and read at 280 nm, using guanidine hydrochloride as the blank.

1.9 - Superoxide Dismutase Activity Assay:

Superoxide dismutase activity was measured in mouse heart homogenates using a Superoxide Dismutase Assay kit (Cayman Chemical, Ann Arbor, MI). Heart samples were homogenized as previously described in the protein carbonyl section. A standard curve was created making dilutions with the SOD standard (bovine erythrocyte SOD

(Cu/Zn). 200 µl of the diluted Radical Detector (tetrazolium salt solution) and 10 µL of Standard (tubes A-G) was added per well in the designated wells on the plate.

For the sample wells, 200 µl of the diluted Radical Detector and 10 µl of sample was added to the wells. Then the reaction was initiated by adding 20 µl of diluted Xanthine Oxidase to all the wells. The wells were shaken for a few seconds to mix and covered with the plate cover. They were incubated on the shaker for 20 minutes at room temperature and absorbance was read at 440-460 nm using a plate reader using a SmartSpec plus spectrophotometer (Bio-Rad, Hercules, CA. SOD activity was calculated using the equation obtained from the linear regression of the standard curve substituting the linearized rate (LR) for each sample. One unit is defined as the amount of enzyme needed to exhibit 50% dismutation of the superoxide radical.

SOD (U/ml) = sample LR - y-intercept x 0.23 ml x sample dilution

2.0 gDNA Extraction:

Genomic DNA was extracted from heart tissue samples using a DNeasy mini kit (Qiagen Inc., Valencia CA). 25 mg of heart tissue for each sample was used and cut into small pieces. Samples were placed in a 1.5 mL microcentrifuge tube with 180 µl Buffer ATL and 20 µl proteinase K. Samples were mixed thoroughly by vortexing, and incubated at 56°C until the tissue is completely lysed. This process took approximately 4 hours. Samples were votexed occasionally during incubation. Next, 200 µl Buffer AL was added to the sample, and mixed thoroughly by vortexing. Then 200 µl ethanol (96–100%) was added and mixed by vortexing. Solution was put into the DNeasy Mini spin column and Centrifuge at 6000 x g for 1 min. Flow through was discarded. Next 500 µl

Buffer AW1 was added, and centrifuged for 1 min at 6000 x g and flow through was discarded. 500 µl Buffer AW1 was added, and centrifuged for 3 minutes at 20,000 x g. Flow through was discarded. 200 µl Buffer AE was pipetted directly onto the DNeasy membrane, incubated at room temperature for 1 min, and then centrifuged for 1 min at 6000 x g to elute.

1.2.2 - gDNA concentration analysis and efficiency determination**:** The samples of DNA were analyzed spectophotometrically for concentration. The absorbance was determined by UV spectroscopy using a SmartSpec plus spectrophotometer (Bio-Rad, Hercules, CA). gDNA was diluted 1:10 in 1X TE buffer, and transferred to a 50 microliter cuvette, using 1X TE buffer as the blank. DNA yield is determined by measuring the concentration of DNA in the eluate by its absorbance at 260 nm. Absorbance readings at 260 nm should fall between 0.1 and 1.0 to be accurate. The concentration of tissue DNA ranged from 0.42-0.89 micrograms DNA/mg tissue.

2.1 Statistical Analysis:

All data were reported as means standard errors. Differences between treatment groups were analyzed using a T-test or One-Way Analysis of Variance (ANOVA) using GraphPad Prism software version 4.0 (GraphPad Software, La Jolla, CA). Significance was accepted at $P<0.05$ level.

Results

Introduction:

Excess nutrients in obesity correlate with an accumulation of oxidant damage [67]. Niacin plays a role in reducing symptoms of high cholesterol, high blood pressure, and diabetes, and could potentially play an antioxidant role in oxidative stress [3]. Adiponectin, initially discovered in 1995 is the most abundant protein hormone secreted from adipose tissue and is involved in regulating glucose levels as well as fatty acid breakdown [88]. Adiponectin was initially thought to be exclusively produced in adipose tissue, but has recently been found in cardiac HL-1 cells [110].

In this study, 32 mice were randomly divided into 2 groups and fed control chow or high-fat diet (HFD) for 6 weeks. After 6 weeks, each diet group was subdivided and treated with either vehicle or niacin in the drinking water for an additional 5 weeks. Total time on diets was 11 weeks. After an 11 week diet, body weights of the HFD group were significantly higher ($p<0.0001$) than the control diets (Figure 1). Niacin treatment had no effect on body weight.

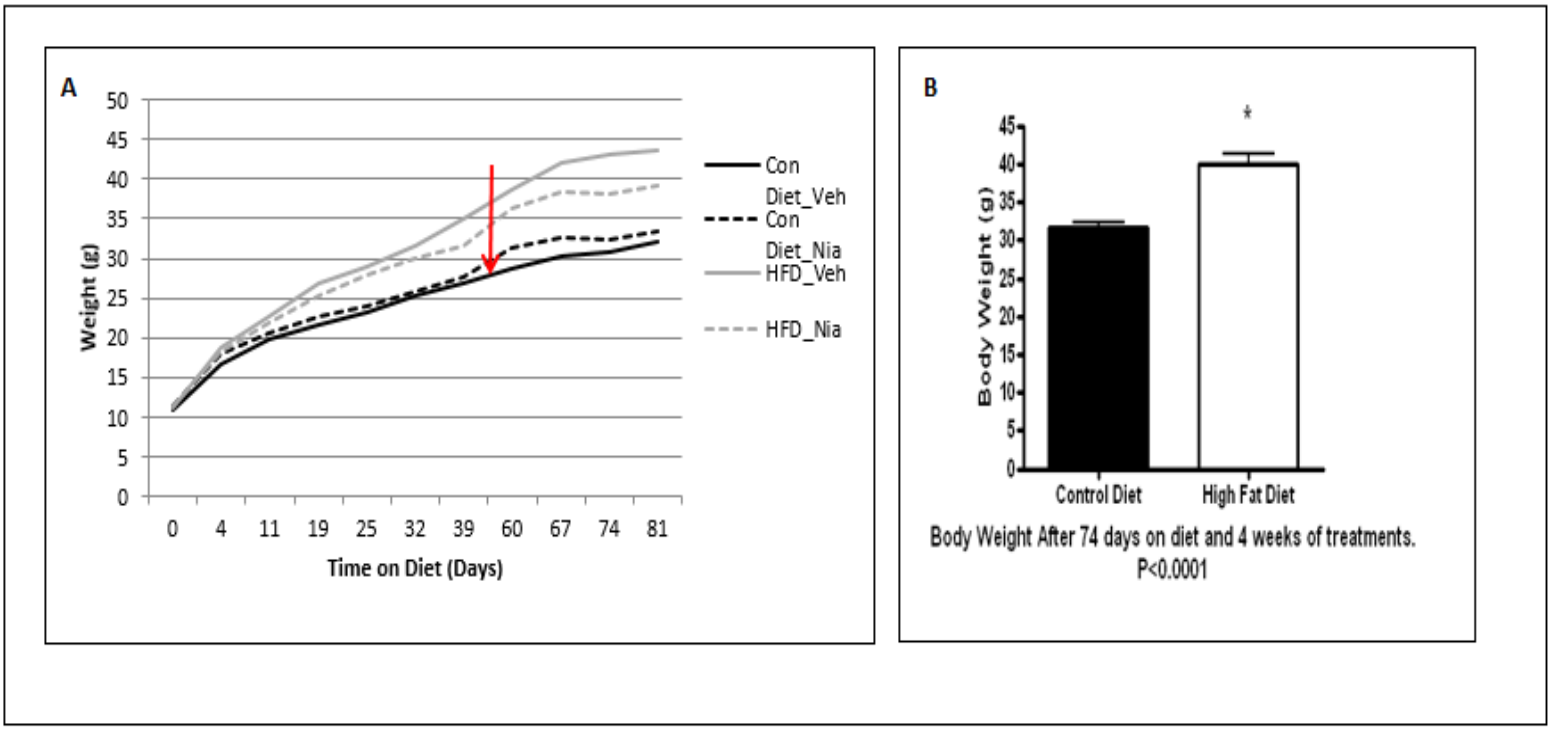

Figure 5: Body weight in mice fed a normal and HFD for 11 weeks. A) Body weights of control group vs. HFD group (*P<.0001). B) Body weights of mice throughout the 11 weeks. The red arrow indicates the time the niacin groups were started on niacin diet (0.3% in water). Solid black line is normal diet, dashed black is normal diet with niacin, and solid gray is high fat diet.

Heart Weight/Body Weight Ratio of High-Fat Diet Compared to Control Group:

At the end of the 11 week experiment period, hearts were rapidly removed, cleaned of any fat, blotted dry and weighed to determine heart weight/body weight ratio. Heart weights in the four groups were not significantly different (Figure 2). Heart weight/body weight ratio was significantly reduced in the high-fat diet mice treated with vehicle or niacin, compared to their normal chow counterparts. This difference was due to an increase in body weight in the high-fat diet groups compared to the normal chow group with no change in heart weight. (Figure 2). Therefore a high-fat diet for 11 weeks has no effect on heart weight but decreased the heart weight/body weight ratio because body weight increased.

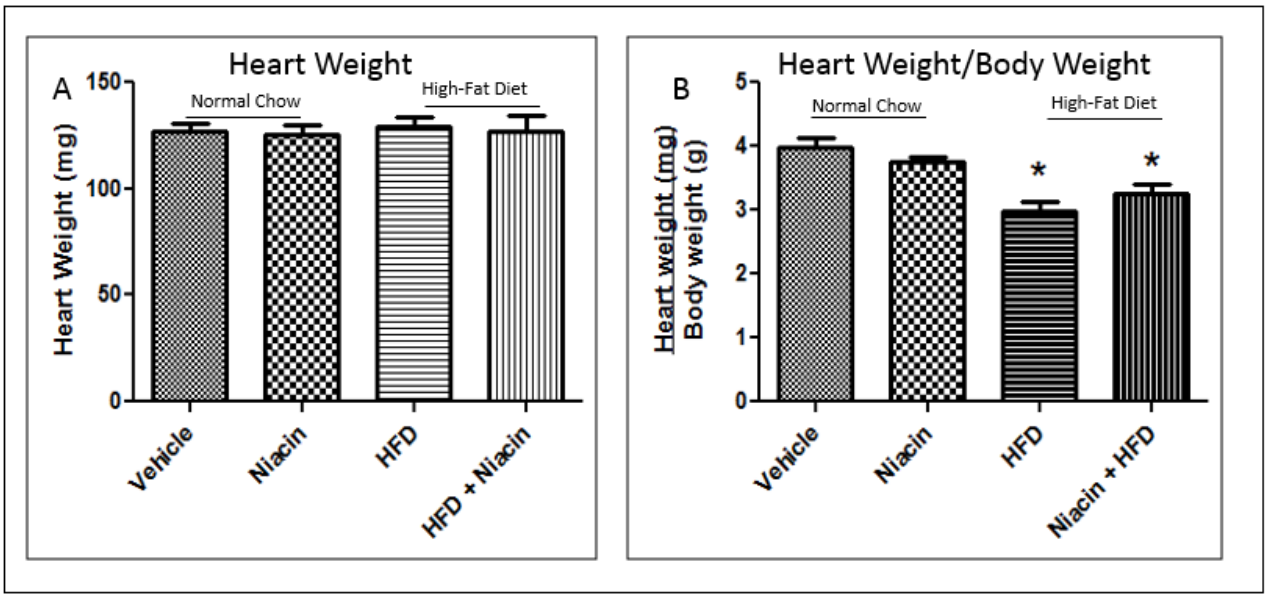

Figure 6: Heart weight and heart weight/body weight ratio in mice fed normal and high-fat diet with vehicle or niacin. Mice were fed either a normal chow or high-fat diet for 11 weeks. During the last 5 weeks each group was treated with vehicle or niacin (0.3%) in drinking water. A) Heart weight (mg tissue) B) Heart weight (mg)/body weight (g) ratio. * indicated significant difference from treatment counter part ($P<0.05$). Data presented represents the mean and standard error (n=6).

Presence of Niacin Receptor GPR109A in the Mouse Heart:

The G-protein-coupled receptor GPR109A binds and is activated by niacin. This receptor has been found to be expressed in various immune cells and highly expressed in adipocytes [112]. To determine whether the message for GPR109A is expressed in the mouse heart, real-time PCR was performed using mouse heart, left ventricle, aorta, kidney, and pericardial fat. RNA was isolated using an RNeasy mini plus kit (Qiagen) and 1 ug of total RNA was reverse transcribed into cDNA using the iScript cDNA synthesis kit. The primers for GPR109A were directed at the mouse niacin receptor 1 (Niacr1) NM_030701. The calculated PCR product size for our GPR109A primers was 178 bp. A band corresponding to PCR product of this length was detected in pericardial fat but not whole heart or left ventricle (Figure 3). Light bands for GPR109A were detected in aorta and kidney. The data suggests that the receptor for niacin, GPR109A is not present in the mouse heart.

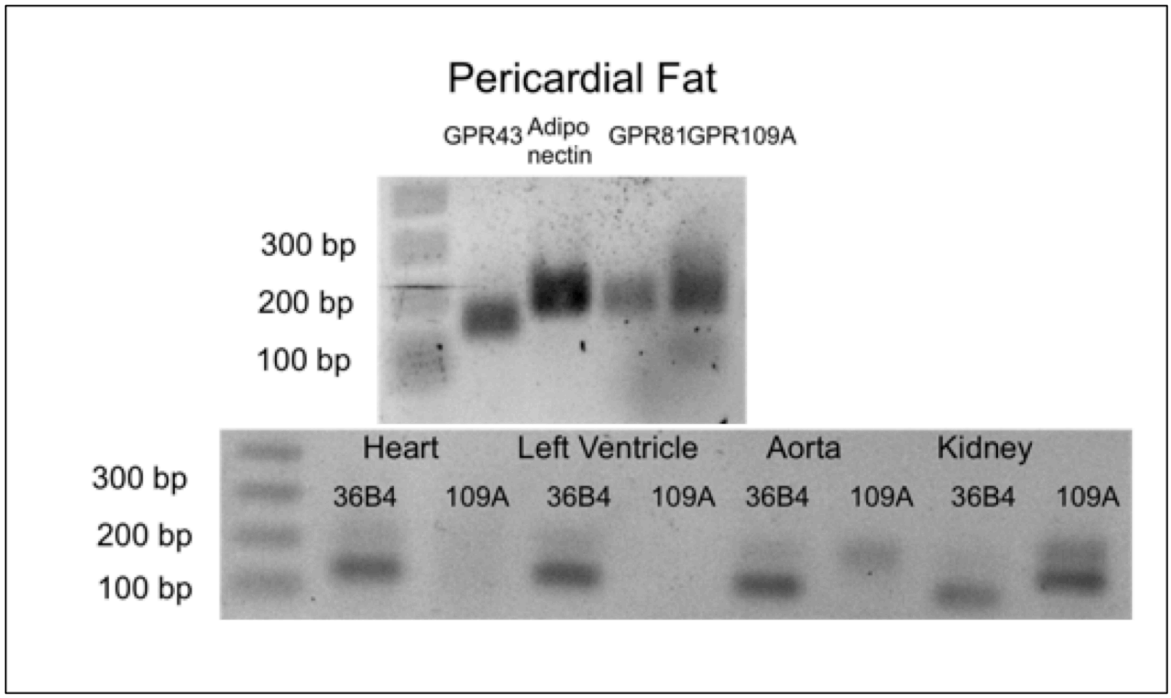

Figure 7: Agarose gel of PCR products to GPR109A. RNA was isolated from whole heart, left ventricle, aorta, kidney, and pericardial fat using RNeasy mini kit plus. cDNA was made using the iScript cDNA synthesis kit using 1 ug total RNA. PCR was performed using 1 uL cDNA, 12.5 uL SYBR green mix, 10.5 uL H2O and forward and reverse GPR109A primers at a final concentration of 0.5 uM. The PCR conditions were an initial denaturation at 95° C for 10 min, followed by 40 cycles of 95° C for 15 seconds, 58° C for 30 seconds and 58° C for 1 minute, then 1 minute at 72° C. 10 uL of each product was combined with 2 uL of gel loading buffer (6x) and run on a 2% agarose gel. The gel was stained with ethidium bromide, and visualized on electrophoresis on a BioRad flour-s multi-imager. 109A refers to GPR109A. 36B4 refers to the housekeeping gene acidic ribosomal phospho-protein P0.

Superoxide Dismutase Activity (SOD) and Protein Carbonylation:

SOD is important in maintaining proper levels of free radicals in the body. The presence of sufficient amounts of the enzyme in cells and tissues typically keeps the concentration of superoxide very low. Quantification of SOD activity is therefore essential in order to fully characterize the antioxidant capabilities of a biological system. A Superoxide Dismutase Assay kit (Cayman Chemical, Ann Arbor, MI) was used to determine SOD levels in the hearts of the mice fed a control and high-fat diet. Xanthine oxidase and hypoxanthine is added to generate superoxide and SOD is calculated by measuring the dismutation of superoxide radicals. Absorbance was read at 440-460 nm using a SmartSpec plus spectrophotometer (Bio-Rad. Hercules, CA). There was no change in levels of SOD activity in the high fat diet group compared to the control group (Figure 4a), indicating no change in oxidative stress levels between the high-fat diet group compared to control.

We next looked at protein carbonyl content in hearts of mice fed a normal and HFD as an indicator of oxidative stress (Cayman's Protein Carbonyl Colorimetric Assay Kit). The kit utilizes 2,4-dinitrophenylhydrazine (DNPH), which will form a hydrazine on carbonylated proteins. The hydrazone can be measured spectophotometrically at an absorbance measured at 370 nm using a SpectraMax Plus microplate reader (Molecular Devices, Palo Alto, CA). The levels of protein carbonylation in the two groups were between 1.4-1.7 nM protein carbonylation per mg of tissue and the high-fat diet group was not significantly different than the control group (Figure 4b).

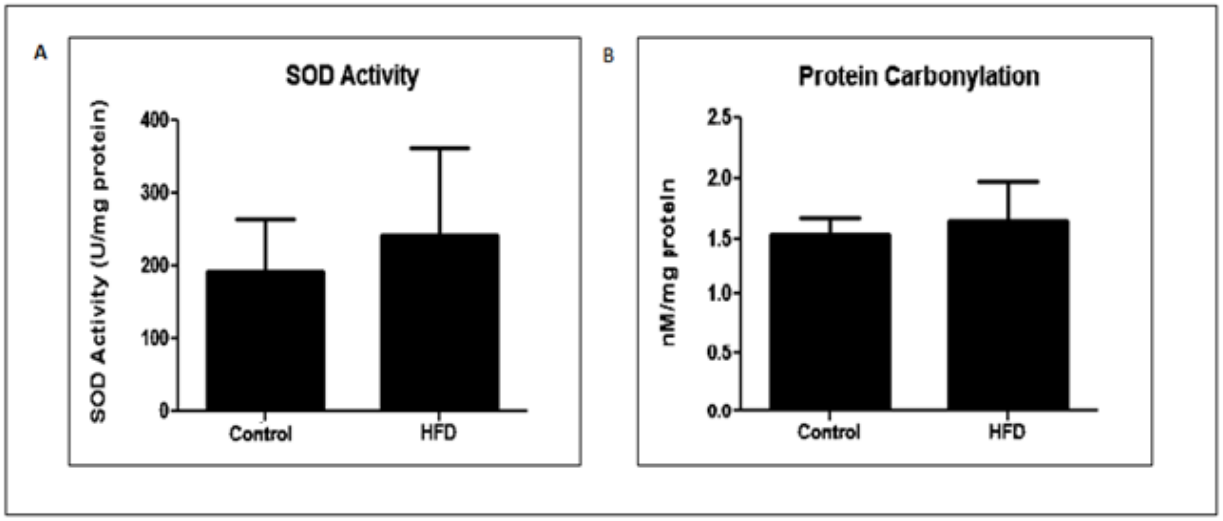

Figure 8: SOD activity (a) and protein carbonylation (b) levels in hearts of mice fed a control and high-fat diet. A) There was no significant increase in the high-fat diet group compared to control group, suggesting that oxidative stress levels in the two groups are similar (n=5) B) Protein carbonylation assay was used to measure protein carbonylation between control and high fat diet group (n=6) by reacting the proteins with DNPH. There was no significant difference in amount of protein carbonylation between the two groups. Data represents mean and standard deviation of the groups.

mRNA Expression of SOD1, SOD2, GPX-1:

SOD1, SOD2, and GPx-1 are endogenous enzymes that regulate oxidative stress levels in the body. In incidents of oxidative stress, these antioxidant enzymes are up-regulated [44]. These experiments were designed to examine antioxidant gene expression in the hearts of mice fed a control and high-fat. In addition, we also examined SOD1, SOD2, and GPx-1 expression in the kidneys of mice fed a control and high-fat diet. In the experiment, 36B4 was used as a housekeeping gene. No difference of expression was observed between groups for 36B4. For these experiments, equal amounts of RNA from each heart was combined for each group in a pooled sample. Expression levels in each group were then expressed as a fold change of expression for the gene compared to the normal chow vehicle treated group (control).

SOD1, SOD2 and GPx-1 expression in the hearts of high-fat diet mice were not different from that of control. Niacin treatment had no effect on expression in mice fed a normal chow (Figure 5a,b). The high-fat diet group treated with niacin had a decreased expression of GPx-1 compared to control group (Figure 5b). A similar analysis was performed on the kidney of control and high-fat diet mice. Similar to that seen with the heart, no change in the expression of SOD1, SOD2, GPx-1 was observed in the kidney (Figure 6). These data suggests that a high-fat diet for 11 weeks did not alter gene expression of SOD1, SOD2, or GPx-1 in the hearts or kidney of mice.

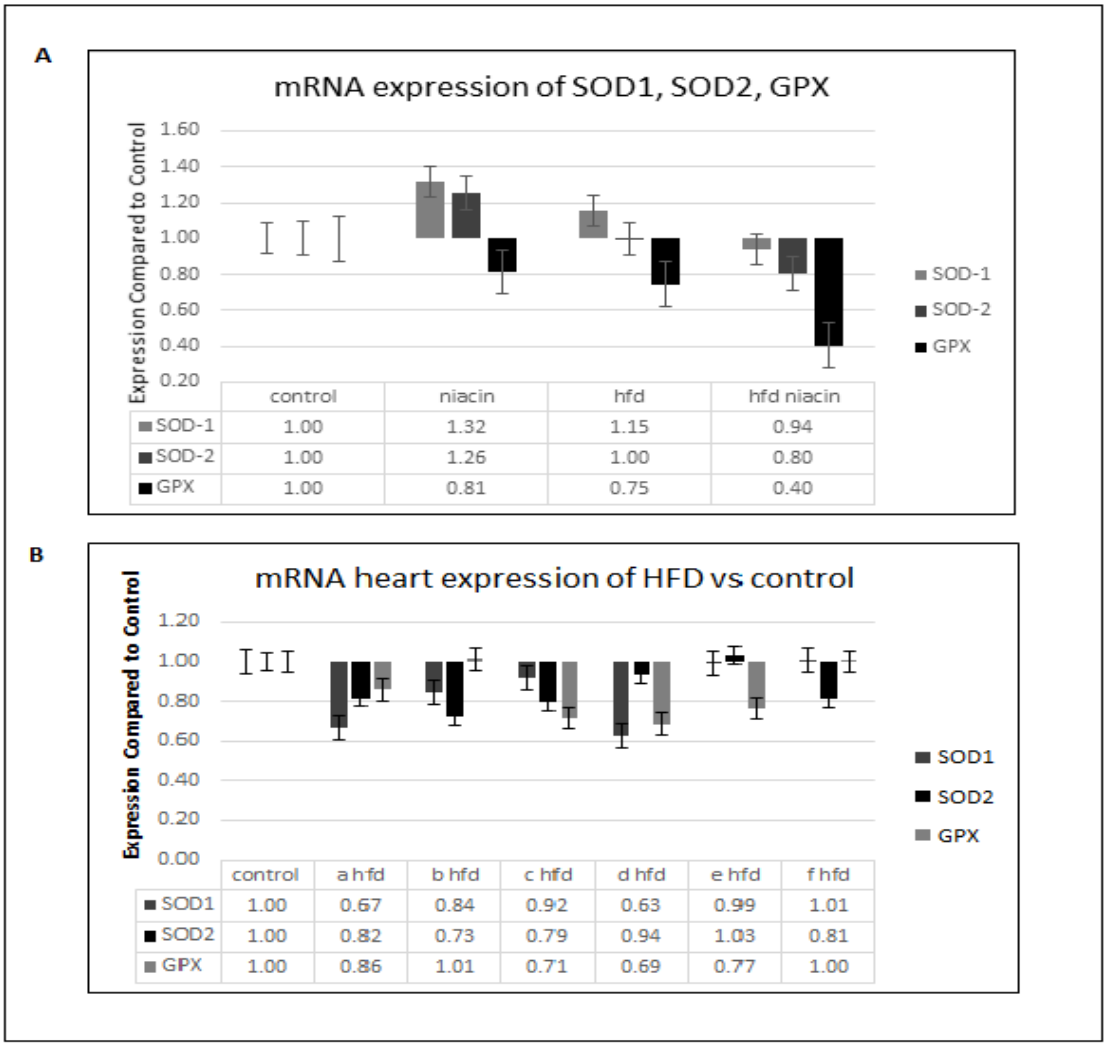

Figure 9: mRNA expression analysis of SOD1, SOD2, and GPx-1 in the heart. One microgram of RNA was isolated and reverse transcribed and used for PCR with primers specific for SOD1, SOD2, and GPx-1. Control group was set to 1. A) SOD1, SOD2 and GPx-1 expression in all four treatment groups. B) mRNA expression analysis of SOD1, SOD2, and GPX in the HFD compared to control. Data represents mean and standard error (n=6). PCR was repeated twice. Expression levels were normalized to 36B4.

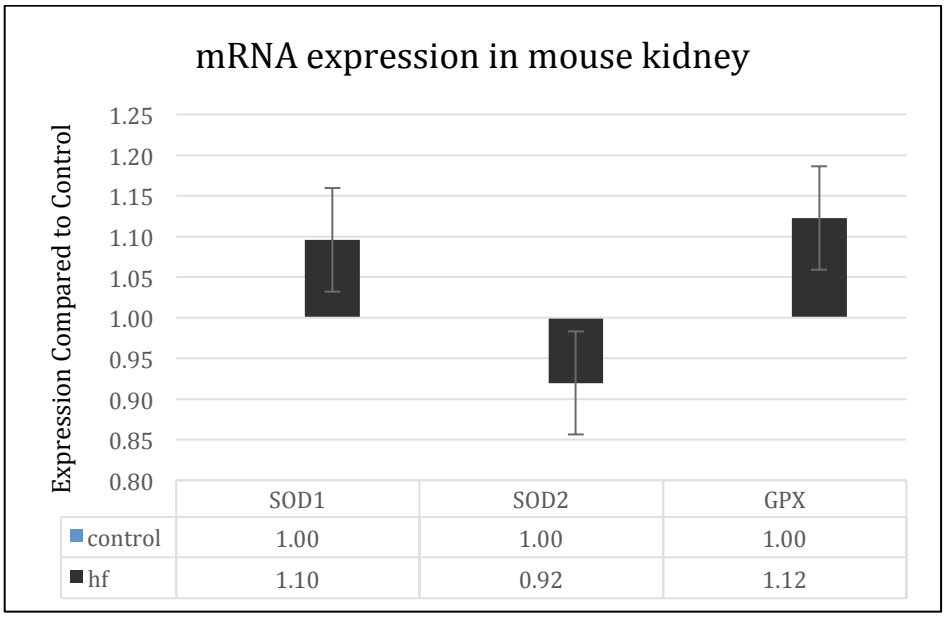

Figure 10: Gene Expression of SOD1, SOD2, and GPx-1 in the kidney of mice fed a normal or high-fat diet for 11 weeks. One microgram of RNA was isolated and reverse transcribed and used for PCR with primers specific for SOD1, SOD2, and GPx-1. Control group was set to 1. Data represents mean and standard error (n=6). PCR was repeated twice. Expression levels were normalized to 36B4.

Expression of SIRT1, SIRT2, and SIRT5:

We next analyzed whether expression of SIRT was altered in the hearts of high-fat diet mice. Sirtuins are a class of deacetylase enzymes that are associated with mechanisms that enhance cellular homeostasis, aid in degenerative disease susceptibility, and are possibly involved with mediating redox stress [3]. Initial experiment examined whether the genes for all 7 isoforms are found in the mouse heart. Real-time PCR analysis revealed that SIRT1, 2, and 5 were present in control hearts but SIRT-3, 4, 6, 7 were not detected with the primers used. We therefore examined whether the expression of SIRT1, SIRT2, and SIRT5 was altered in the hearts of mice fed a high-fat diet. Figure 9 depicts SIRT1, 2, and 5 expression in all for groups of mice. SIRT2 expression did not change across any of the groups. Mice fed a high-fat diet have elevated expression of SIRT5 in the heart as did control mice treated with niacin. High-fat diet mice on niacin had levels of SIRT1, 2, and 5 that were not different from mice fed normal chow (Figure 7).

To determine whether protein expression of SIRT1 followed the same pattern as gene expression, western blot analysis was performed using polyclonal rabbit anti-sirt1, and polyclonal mouse anti-actin primary antibodies (Millipore, Billerica, MA). SIRT1 western blot analysis did not show an increase of expression in the high-fat diet compared to control group. Expression of SIRT1 was elevated in the niacin treated groups compared to their vehicle counterparts (Figure 8).

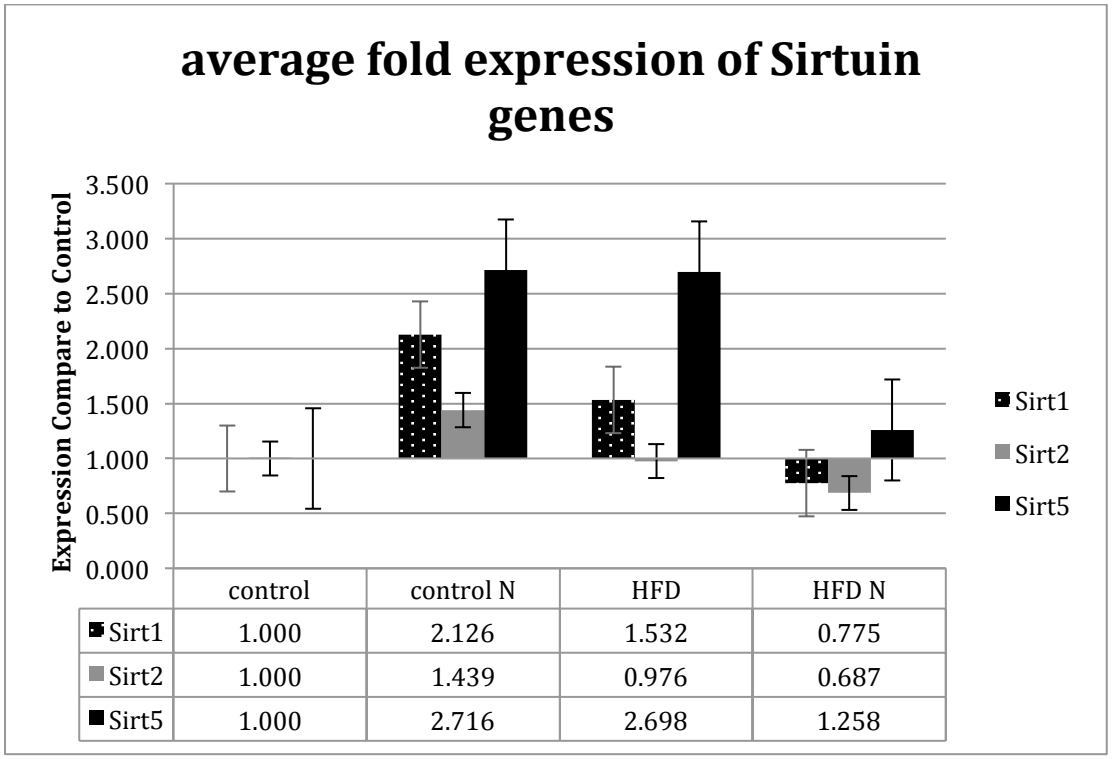

	control	control N	HFD	HFD N
Sirt1	1.000	2.126	1.532	0.775
Sirt2	1.000	1.439	0.976	0.687
Sirt5	1.000	2.716	2.698	1.258

Figure 11: Real-time PCR of sirt1, sirt2, and sirt5 in the heart of mice from all four experiment groups. Graph represents average mRNA expression fold change compared to control group. One microgram of RNA was isolated and reverse transcribed and used for PCR with primers specific for SOD1, SOD2, GPX-1. Sirt 1 and sirt5 expression increases in control group fed niacin and in high fat diet group. Data represents mean and standard error for five mice in each group. PCR was repeated two times (n=5). Expression levels were normalized to the housekeeping gene, 36B4.

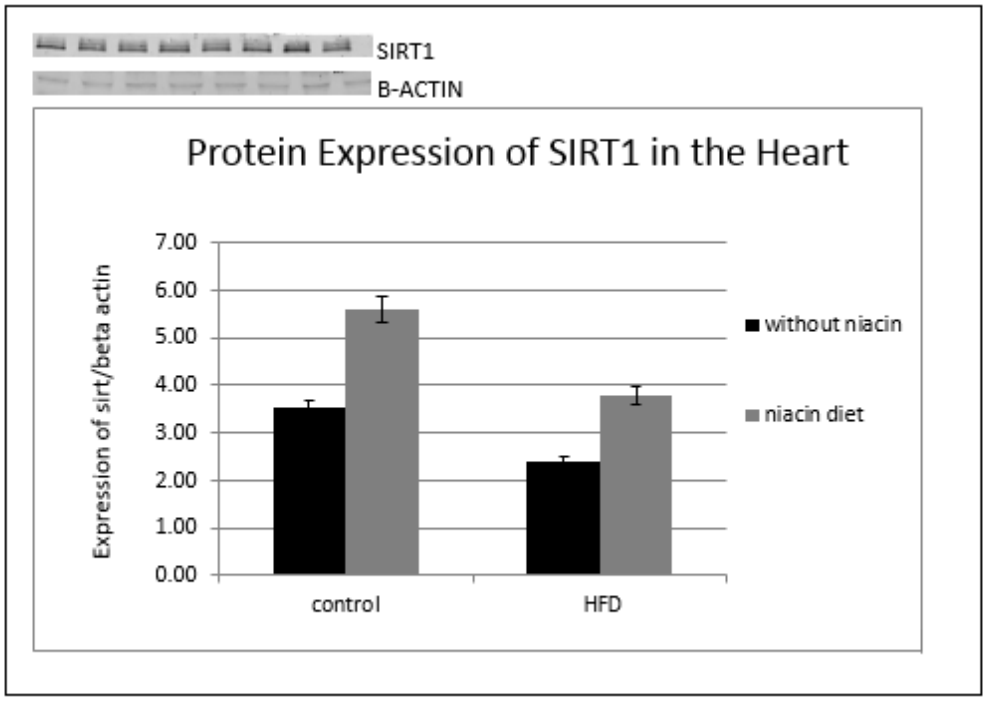

Figure 12: Western blot analysis of sirt1 in the heart. Protein expression is slightly higher in the high-fat diet group fed niacin when compared to the high-fat diet that was not fed niacin. The control diet fed niacin is slightly higher than the control group without niacin. Data represents mean and standard error (n=3). Sirt1 values were normalized to actin.

Adiponectin Expression in the Mouse Heart:

Along with energy storage, adipose tissue functions as an endocrine organ secreting numerous molecules that can affect metabolism. For many years adiponectin was thought to be exclusively secreted by adipose tissue, but evidence suggest adiponectin is also expressed in cardiomyocytes and epicardial adipose tissue [94, 95]. Cardiomyocyte derived adiponectin directly regulates cardiac metabolism by AMPK activation via cardiac AdipoR1 and AdipoR1 [96]. Since there is some controversy as to whether adiponectin can be synthesized in cardiomyocytes, we wanted to see if adiponectin is being produced in the mouse hearts and whether its expression was regulated by diet. Western blots were performed using rabbit polyclonal antibodies for adiponectin (Abcam, Cambridge, MA). Mouse pericardial fat was used as a positive control. A Licor Odyssey imager was used to detect the immunoreactive bands. Blots were analyzed using the Odyssey Software v2.0. Beta-actin was run as a loading control protein, and protein levels were standardized to beta-actin levels. Adiponectin protein expression was shown in the heart for all four groups (Figure 9). Protein expression was significantly lower in the high-fat diet compared to the control group ($p<0.05$). This data suggests that adiponectin is expressed in the mouse heart, and protein expression is down-regulated in the high-fat diet.

Adiponectin PCR product was 100% matching adiponectin sequence (MWG Operon). Real-time PCR analysis suggests that adiponectin is being produced in the heart. There is a slight increase in expression of adiponectin in the high-fat mouse heart group compared to the control group (Figure 10).

In addition to examining adiponectin mRNA expression, real-time PCR of adiponectin receptors AdipoR1 and AdipoR2 were expressed in the mouse heart tissue, but did not vary in expression levels between the four groups (Figure 11). Peroxisome proliferator-activated receptor γ (PPARγ), which is shown to increase adiponectin expression when activated [93], showed no change in mRNA expression in any of the groups compared to control (Figure 12).

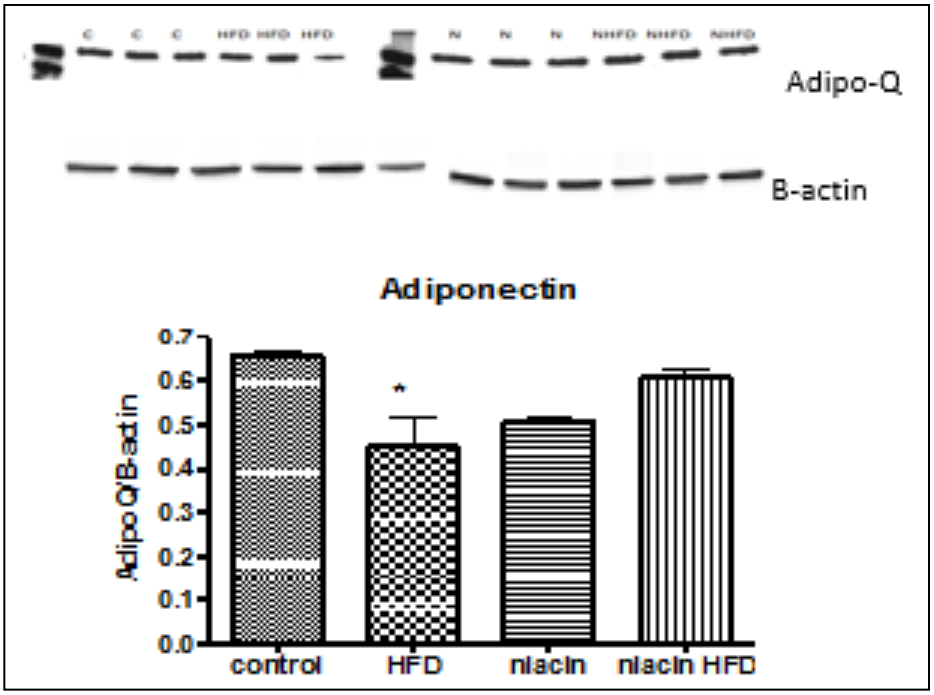

Figure 13: Western blot analysis of adiponectin on mouse heart tissue. Protein expression of adiponectin in the hearts of all four groups was analyzed using western blot analysis with rabbit polyclonal antibody for adiponectin. The HFD treatment group had a significantly lower protein expression than the control group. Adiponectin levels were normalized to actin. (*P<0.05). Western blot was repeated three times.

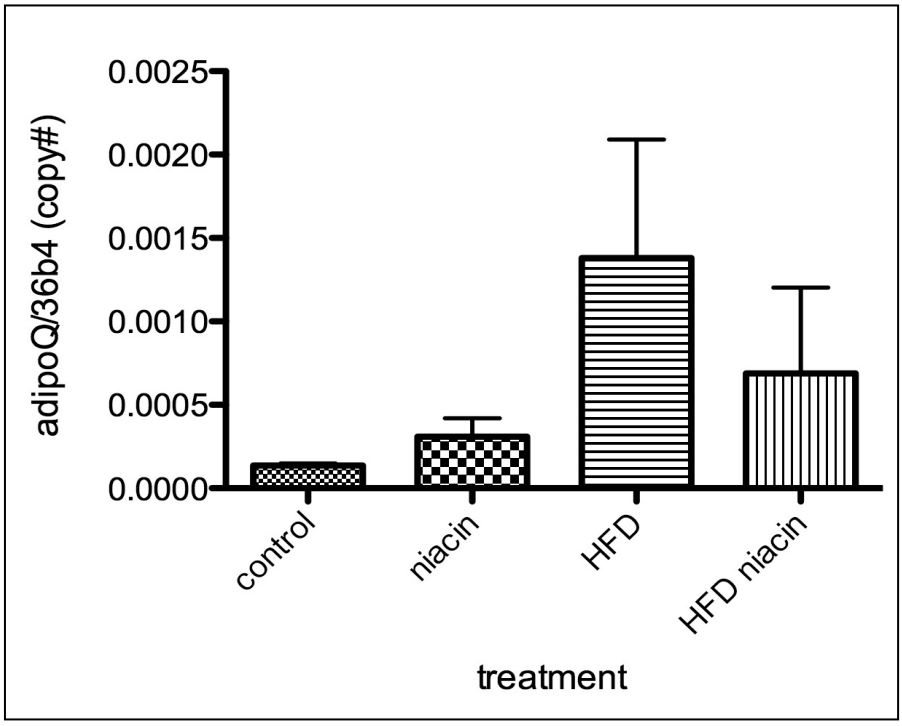

Figure 14: Copy number of adiponectin from RT-PCR was determined in the four treatment groups. 500 nanograms of RNA was isolated and reverse transcribed and used for PCR with primers specific for adiponectin. There is a slight increase in copy number of adiponectin in the high-fat diet but was not statistically significant. Data represents mean and standard error (n=6). PCR was repeated twice. Expression levels were normalized to 36B4.

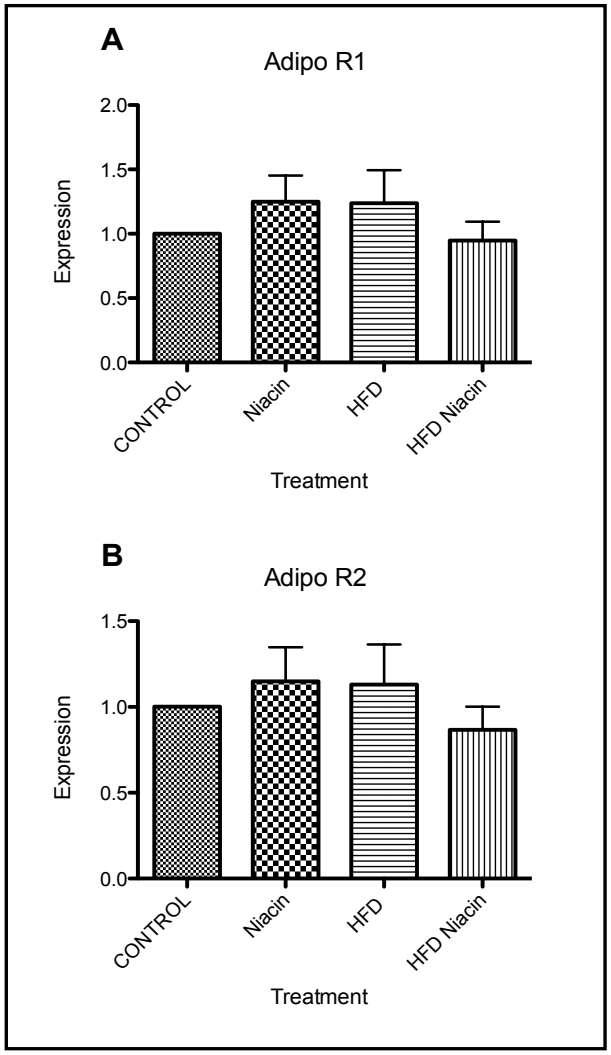

Figure 15: mRNA expression of adipo R1 and adipo R2 in the mouse heart. 500 nanograms of RNA was isolated and reverse transcribed and used for PCR with primers specific for adipo R1 and adipo R2. There was no significant difference in expression levels of any group compared to control. Data represents mean and standard error (n=5). PCR was repeated twice. Expression levels were normalized to 36B4.

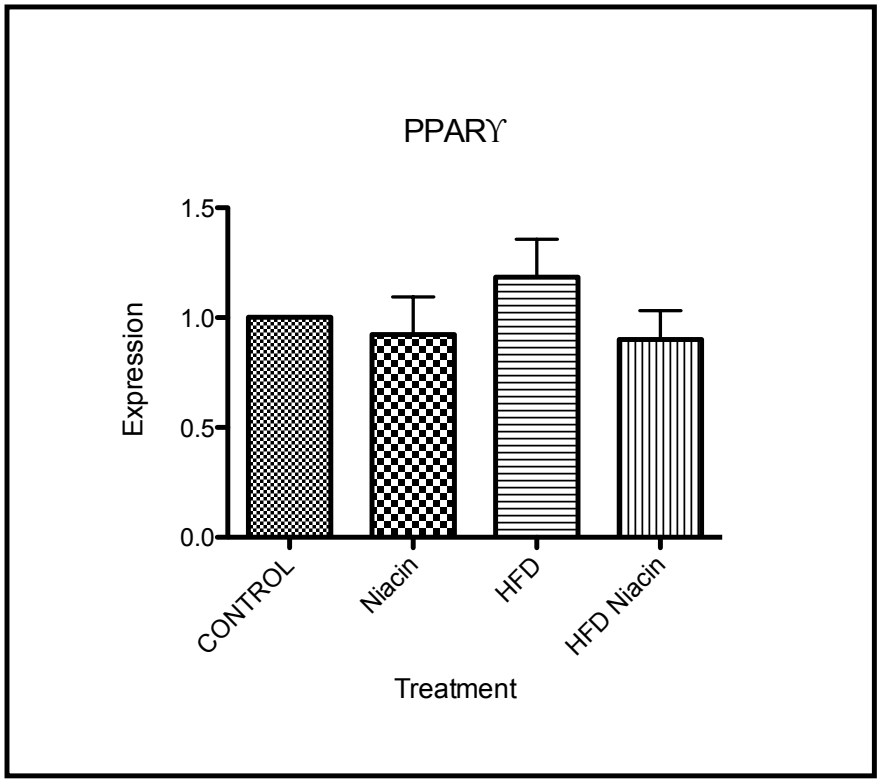

Figure 16: mRNA expression of PPARγ in the mouse heart. 500 nanograms of RNA was isolated and reverse transcribed and used for PCR with primers specific for PPARγ. There was no significant change in expression levels of any group compared to control. Data represents mean and standard error (n=5). PCR was repeated twice. Expression levels were normalized to 36B4.

Discussion

Oxidative Stress in the Mouse Heart

Oxidative stress is a contributing factor in the progression of multiple diseases including stroke, hypertension, diabetes mellitus, neurodegeneration, aging, and cardiovascular disease [1]. Obesity can cause oxidative stress due to accumulation of excess nutrients leading to an increase in free radicals. Obesity is a strong risk factor for developing dyslipidemia, diabetes mellitus, and cardiovascular diseases such as heart failure (HF), coronary heart disease (CHD), hypertension, and atherosclerosis. Previous studies in mice have shown that a high-fat diet can lead to oxidative stress in the heart [55]. The objective of our study was to determine if an eleven-week high-fat diet would trigger oxidative stress and lead to any signs of heart failure. For our study, we used 57BL/6 mice (n=32). Mice were weighed and randomly separated into two groups, where they were fed a control (10% kcal as fat) or high fat (60% kcal as fat) diet for 6 weeks. After 6 weeks on their respectable diets, mice on control and high fat diet were given vehicle (n=8) or 0.3% niacin (n=8) in water, and were treated for 5 additional weeks. At the end of the treatment periods, mice were decapitated, and the hearts and kidneys were frozen in liquid nitrogen and stored at -80° C.

The mice fed the high-fat diet had a significant increase in body weight compared with the control group ($P<0.0001$). However, the heart weights of the high-fat diet group compared to control group did not differ, and the heart weight/body weight ratio was not indicative of possible heart failure/hypertrophy. Previous studies that treated mice with a 45% high-fat have shown that, along with oxidative stress, heart weights of high-fat diet group increases significantly compared to control group [85]. In that study, 14 weeks was long enough to show a significant increase in heart weight in the high-fat group, compared to the control group. This suggests that an 11 week high-fat diet may not be long enough to show signs of heart failure.

The possibility of oxidative stress due to a high-fat diet was examined next. Protein carbonylation content, an indicator or oxidative stress, was measured in the hearts from the high-fat and control group. Cellular proteins are believed to be a target of free radicals, and accumulation of oxidized proteins can impair cellular function [113]. After measuring protein carbonyl content, we found that hearts from the high-fat diet group were not significantly different compared to control group. SOD activity was also measured. Quantification of SOD is essential in order to fully characterize the antioxidant capabilities of a biological system. Similar to protein carbonylation, we found no increase in SOD activity in high-fat diet hearts compared to control, indicating there was no increase in superoxide levels. These data suggest the mice hearts from the high-fat group did not undergo oxidative stress.

When the balance between ROS production and antioxidant defense is lost, oxidative stress occurs. Through a series of events, oxidative stress deregulates the cellular functions leading to various pathological conditions, including conditions relating

to the heart. An effective mechanism to prevent the free radical induced tissue cell damage is accomplished by a set of endogenous antioxidant enzymes like SOD1, SOD2, and GPx-1. Enzymatic activity become elevated to balance the level of free radicals. Therefore, using RT-PCR analysis, we analyzed the possible changes in expression for SOD1, SOD2, and GPx-1 on control and high-fat diet mouse hearts and kidneys. Mouse hearts from high-fat diet group had the same level of expression of SOD1, SOD2, and GPx-1 compared to the control group. Kidneys from high-fat diet group were also similar to the control group. Data from antioxidant gene expression along with protein carbonylation and SOD activity indicates that mouse hearts from high-fat diet groups did not undergo oxidative stress compared to the control group. We expected to see an increase in oxidative stress in the high-fat diet group, which would have allowed us to study gene expression and effects of niacin on high-fat diet. Figuring out exactly when the buildup of free radicals from nutrient excess elicits an oxidative stress response is important in understanding the exact role of a high-fat diet in cardiovascular oxidative stress.

Although diets vary in content and length, previous research has shown that a high-fat diet in mice does induce oxidative stress, and cause an increase in endogenous antioxidant enzymes in the heart. There are few studies that examine oxidative stress in the hearts of obese rodents, but experiments that have been successful in inducing oxidative stress used a longer diet time. One study used eight-week old C57BL/6 mice on a twenty-two-week high-fat diet of 45%, compared to a twenty-two week control diet (5% fat). Impaired left ventricular ejection fraction (LVEF), enhanced left ventricle (LV) remodeling, inflammation, fibrosis, oxidative stress and apoptosis was found in the high-

fat group compared to the control [85]. Another study did a sixteen-week high-fat diet on white albino rats [55]. The heart, kidney, and liver of the high-fat diet group had increased oxidative stress compared to the control group.

In conclusion, an eleven week high-fat diet did not induce oxidative stress in the mouse heart or kidney. Elevated levels of oxidative stress have been shown to be a precursor in heart failure, and obesity can cause or exacerbate this process. Eleven weeks may not have been a sufficient amount of time to initiate a cascade of problems, including oxidative stress and hypertrophy, which can ultimately lead to heart conditions.

SIRT1 and SIRT5 Expression

Sirtuins are a class of deacetylase enzymes that are associated with mechanisms that enhance cellular homeostasis, aid in degenerative disease susceptibility, and are involved with mediating redox stress. Examining expression of various sirtuin genes could provide insight to levels of redox stress in the high-fat diet hearts compared to control group. Real-time PCR showed an increase in expression of SIRT1 and SIRT5 in the high-fat diet and in the control diet fed niacin. Activation of SIRT1 in cardiomyocytes have been shown to protect the heart from heart failure, decreasing the amount of oxidative stress, cardiac hypertrophy, apoptosis, and cardiac dysfunction in transgenic mouse hearts [8]. It is known that SIRT1 can alleviate oxidative stress by elevating antioxidant levels of SOD through FOXO-dependent mechanisms [62]. In contrast to mRNA expression, SIRT 1 western blot analysis did not

show an increase in the high-fat group compared to control. Furthermore, the high-fat diet group treated with niacin had increased SIRT1 protein expression compared to the high-fat diet group without niacin, and the control group treated with niacin had increased protein expression compared to the group on a control diet without niacin. Effects of niacin on SIRT1 expression in the heart have not yet been studied, but our data suggests that an increase in protein expression of the niacin groups may be due to niacin playing a protective role in the heart by activating SIRT1.

Effects of Niacin

Niacin is a vitamin that plays a role in reducing symptoms of high cholesterol, high blood pressure, and diabetes, and could potentially play an antioxidant role in oxidative stress [114]. The purpose of our study was to examine oxidative stress in mouse hearts that were fed a high-fat diet, and to study any potential antioxidant effects of niacin. Niacin binds to a G-coupled protein receptor called GPR109A. The binding of niacin stimulates the receptor and causes the inhibition of fat breakdown. This receptor has been found to be expressed in various immune cells and highly expressed in adipocytes [112]. Real-time PCR analysis was run on mouse heart, left ventricle, aorta, kidney, and pericardial fat with a GPR109A primer, and pericardial fat was used as a positive control. PCR products were then analyzed using a 2% agarose gel. There was no band for GPR109A in the mouse heart or left ventricle, but there was a very faint band for the aorta and kidney. This suggests that GPR109A is not expressed in the mouse heart, but could possibly be expressed in low concentrations in the kidney and aorta. It is possible that the mice aorta expresses GPR109A in its endothelial cells. In

a study using human aortic endothelial cells, niacin increased NADPH and reduced Gpx-1 levels and LDL oxidation [68].

Expression of antioxidant genes and oxidative stress markers did not vary in the hearts of the niacin treated groups compared to vehicle groups. This could be from of a lack of the niacin receptor GPR109A in the heart; therefore, niacin does not directly affect oxidative stress in the heart. However, this needs to be investigated further, considering the high-fat diet group also did not show signs of oxidative stress.

Adiponectin Expression in the Mouse Heart

For many years adiponectin was assumed to be secreted exclusively by adipose tissue, but recent research has found adiponectin to be expressed in cardiomyocytes and epicardial adipose tissue [110]. Our research wanted to examine adiponectin expression in the mouse heart, and look at the possible variation of expression between high-fat diet and control diet. Adiponectin expression was present in the hearts of all treatment groups. There was a decrease in protein levels in the high-fat diet group compared to the control, while mRNA expression of adiponectin was slightly higher in the high-fat diet compared to control, although not significant. Mice from the 14-week high-fat diet experiment mentioned previously had a significant decreased in mRNA expression of adiponectin in the hearts of the 14 and 22 week groups compared to control group [85]. This suggests the possibility that a longer high-fat diet is needed to see a significant change in mRNA expression of adiponectin. Adiponectin in adipose tissue is typically lower in obese individuals [103]. Our western blot analysis correlates

with previous research, showing a significant decrease in adiponectin of the high-fat diet group compared to control. Adiponectin being produced in the heart could be playing a more direct role in the progression of CVD compared to circulating adiponectin.

When activated, PPAR-γ increases adiponectin gene expression, production and secretion [48]. However, there was no change in expression of PPAR-γ in the hearts of the high-fat diet compared to control, which would explain why we found no significant increase in the mRNA expression of adiponectin in the high-fat diet group compared to control. Adiponectin receptors AdipoR1 and AdipoR2 were also studied using RT-PCR. Expression of these receptors was found in the mouse heart, no significant difference in expression was found between the four groups. Our data suggests that adiponectin is being produced in the heart, and could potentially be eliciting a local response, along with circulating adiponectin. It is possible that repeating the same experiment with a longer diet would show changes in expression of adiponectin, AdipoR1, AdipoR1 and PPAR-γ in the high-fat diet compared to control.

Conclusion

Mice fed the high fat diet had significantly increased body weights ($p<0.0001$). There was no significant change in expression of SOD-1, SOD-2, or GPx-1 in the hearts between four treatment groups. There was also no change in SOD activity or protein carbonylation in the hearts of mice fed a high-fat diet compared to control group. An increase in the gene expression of SIRT1 and SIRT5 was seen in the high fat diet compared to normal diet. Niacin alone also caused an increase in SIRT1 gene expression. Expression of SIRT1 and SIRT5 in the hearts of the high fat diet treated with niacin were not significantly different from control group. Niacin treated groups had an increase in SIRT1 protein expression compared to the counterpart vehicle group.

In conclusion, mice on a high fat diet for 11 weeks did not show alterations in antioxidant gene expression, SOD activity or protein carbonylation. Increases in mRNA expression of in SIRT1 and SIRT5 in the high-fat and niacin diets, and increased SIRT1 protein expression in niacin treated hearts could be due to a protective role against oxidative stress.

Adiponectin protein and mRNA expression was found in the mouse hearts. Adiponectin protein expression was significantly lower ($p<0.05$) in the high-fat diet hearts compared to control. Our data suggests that adiponectin is being produced in the mouse heart, and could be eliciting a local response, along with the circulating adiponectin.

References

1. Minino, A.M., et al., *Death in the United States, 2007.* NCHS Data Brief, 2009(26): p. 1-8.
2. Marsden, P.A., et al., *Structure and chromosomal localization of the human constitutive endothelial nitric oxide synthase gene.* J Biol Chem, 1993. **268**(23): p. 17478-88.
3. Kamanna, V.S. and M.L. Kashyap, *Mechanism of action of niacin.* Am J Cardiol, 2008. **101**(8A): p. 20B-26B.
4. Verdin, E., et al., *Sirtuin regulation of mitochondria: energy production, apoptosis, and signaling.* Trends Biochem Sci, 2010. **35**(12): p. 669-75.
5. Dandona, P., et al., *Metabolic syndrome: a comprehensive perspective based on interactions between obesity, diabetes, and inflammation.* Circulation, 2005. **111**(11): p. 1448-54.
6. Savini, I., et al., *Obesity-associated oxidative stress: strategies finalized to improve redox state.* Int J Mol Sci, 2013. **14**(5): p. 10497-538.
7. Hubert, H.B., et al., *Obesity as an independent risk factor for cardiovascular disease: a 26-year follow-up of participants in the Framingham Heart Study.* Circulation, 1983. **67**(5): p. 968-77.
8. Haigis, M.C. and L.P. Guarente, *Mammalian sirtuins--emerging roles in physiology, aging, and calorie restriction.* Genes Dev, 2006. **20**(21): p. 2913-21.
9. Castro, L. and B.A. Freeman, *Reactive oxygen species in human health and disease.* Nutrition, 2001. **17**(2): p. 161, 163-5.
10. Wanders, D., E.P. Plaisance, and R.L. Judd, *Lipid-lowering drugs and circulating adiponectin.* Vitam Horm, 2012. **90**: p. 341-74.
11. Nunn, A.V., J.D. Bell, and G.W. Guy, *Lifestyle-induced metabolic inflexibility and accelerated ageing syndrome: insulin resistance, friend or foe?* Nutr Metab (Lond), 2009. **6**: p. 16.
12. Martinez, J.A., *Mitochondrial oxidative stress and inflammation: an slalom to obesity and insulin resistance.* J Physiol Biochem, 2006. **62**(4): p. 303-6.
13. Bondia-Pons, I., L. Ryan, and J.A. Martinez, *Oxidative stress and inflammation interactions in human obesity.* J Physiol Biochem, 2012. **68**(4): p. 701-11.
14. Droge, W., *Free radicals in the physiological control of cell function.* Physiol Rev, 2002. **82**(1): p. 47-95.
15. Picard, F., et al., *Sirt1 promotes fat mobilization in white adipocytes by repressing PPAR-gamma.* Nature, 2004. **429**(6993): p. 771-6.
16. Planavila, A., et al., *Sirt1 acts in association with PPARalpha to protect the heart from hypertrophy, metabolic dysregulation, and inflammation.* Cardiovasc Res, 2011. **90**(2): p. 276-84.

17. Chong, Z.Z., et al., *Targeting cardiovascular disease with novel SIRT1 pathways.* Future Cardiol, 2012. **8**(1): p. 89-100.
18. Webster, B.R., et al., *The role of sirtuins in modulating redox stressors.* Free Radic Biol Med, 2012. **52**(2): p. 281-90.
19. Alcendor, R.R., et al., *Sirt1 regulates aging and resistance to oxidative stress in the heart.* Circ Res, 2007. **100**(10): p. 1512-21.
20. Alfadda, A.A. and R.M. Sallam, *Reactive oxygen species in health and disease.* J Biomed Biotechnol, 2012. **2012**: p. 936486.
21. Bae, Y.S., et al., *Regulation of reactive oxygen species generation in cell signaling.* Mol Cells, 2011. **32**(6): p. 491-509.
22. Mollnau, H., et al., *Effects of angiotensin II infusion on the expression and function of NAD(P)H oxidase and components of nitric oxide/cGMP signaling.* Circ Res, 2002. **90**(4): p. E58-65.
23. Adamczyk, A., A. Kazmierczak, and J.B. Strosznajder, *Alpha-synuclein and its neurotoxic fragment inhibit dopamine uptake into rat striatal synaptosomes. Relationship to nitric oxide.* Neurochem Int, 2006. **49**(4): p. 407-12.
24. Matsumoto, H., et al., *Nitric oxide is an initiator of intercellular signal transduction for stress response after hyperthermia in mutant p53 cells of human glioblastoma.* Cancer Res, 1999. **59**(13): p. 3239-44.
25. Orlando, G.F., G. Wolf, and M. Engelmann, *Role of neuronal nitric oxide synthase in the regulation of the neuroendocrine stress response in rodents: insights from mutant mice.* Amino Acids, 2008. **35**(1): p. 17-27.
26. Mander, P. and G.C. Brown, *Activation of microglial NADPH oxidase is synergistic with glial iNOS expression in inducing neuronal death: a dual-key mechanism of inflammatory neurodegeneration.* J Neuroinflammation, 2005. **2**: p. 20.
27. Ohta, Y., et al., *Xanthine oxidase-derived reactive oxygen species contribute to the development of D-galactosamine-induced liver injury in rats.* Free Radic Res, 2007. **41**(2): p. 135-44.
28. Pacher, P., A. Nivorozhkin, and C. Szabo, *Therapeutic effects of xanthine oxidase inhibitors: renaissance half a century after the discovery of allopurinol.* Pharmacol Rev, 2006. **58**(1): p. 87-114.
29. Berendes, H., R.A. Bridges, and R.A. Good, *A fatal granulomatosus of childhood: the clinical study of a new syndrome.* Minn Med, 1957. **40**(5): p. 309-12.
30. Emmendorffer, A., et al., *Production of oxygen radicals by fibroblasts and neutrophils from a patient with x-linked chronic granulomatous disease.* Eur J Haematol, 1993. **51**(4): p. 223-7.
31. Johnston, R.B., Jr., et al., *The role of superoxide anion generation in phagocytic bactericidal activity. Studies with normal and chronic granulomatous disease leukocytes.* J Clin Invest, 1975. **55**(6): p. 1357-72.
32. Friis, M.B., K.G. Vorum, and I.H. Lambert, *Volume-sensitive NADPH oxidase activity and taurine efflux in NIH3T3 mouse fibroblasts.* Am J Physiol Cell Physiol, 2008. **294**(6): p. C1552-65.

33. Xu, H., et al., *Differential roles of PKCalpha and PKCepsilon in controlling the gene expression of Nox4 in human endothelial cells.* Free Radic Biol Med, 2008. **44**(8): p. 1656-67.
34. Lyle, A.N. and K.K. Griendling, *Modulation of vascular smooth muscle signaling by reactive oxygen species.* Physiology (Bethesda), 2006. **21**: p. 269-80.
35. Lassegue, B., et al., *Novel gp91(phox) homologues in vascular smooth muscle cells : nox1 mediates angiotensin II-induced superoxide formation and redox-sensitive signaling pathways.* Circ Res, 2001. **88**(9): p. 888-94.
36. Foster, D.B., et al., *Redox signaling and protein phosphorylation in mitochondria: progress and prospects.* J Bioenerg Biomembr, 2009. **41**(2): p. 159-68.
37. Das, D.K., et al., *Reactive oxygen species function as second messenger during ischemic preconditioning of heart.* Mol Cell Biochem, 1999. **196**(1-2): p. 59-67.
38. Katoh, S., et al., *Hyperoxia induces the neuronal differentiated phenotype of PC12 cells via a sustained activity of mitogen-activated protein kinase induced by Bcl-2.* Biochem J, 1999. **338 (Pt 2)**: p. 465-70.
39. Sauer, H., et al., *Effects of electrical fields on cardiomyocyte differentiation of embryonic stem cells.* J Cell Biochem, 1999. **75**(4): p. 710-23.
40. Ruiz-Gines, J.A., et al., *Reactive oxygen species induce proliferation of bovine aortic endothelial cells.* J Cardiovasc Pharmacol, 2000. **35**(1): p. 109-13.
41. Burdon, R.H. and C. Rice-Evans, *Free radicals and the regulation of mammalian cell proliferation.* Free Radic Res Commun, 1989. **6**(6): p. 345-58.
42. Rao, G.N. and B.C. Berk, *Active oxygen species stimulate vascular smooth muscle cell growth and proto-oncogene expression.* Circ Res, 1992. **70**(3): p. 593-9.
43. Wartenberg, M., et al., *Growth stimulation versus induction of cell quiescence by hydrogen peroxide in prostate tumor spheroids is encoded by the duration of the Ca(2+) response.* J Biol Chem, 1999. **274**(39): p. 27759-67.
44. Halliwell, B., *Antioxidant defence mechanisms: from the beginning to the end (of the beginning).* Free Radic Res, 1999. **31**(4): p. 261-72.
45. Medina-Navarro, R., et al., *Protein antioxidant response to the stress and the relationship between molecular structure and antioxidant function.* PLoS One, 2010. **5**(1): p. e8971.
46. Yasuno, S., et al., *Impact of type 2 diabetes and coronary heart disease on cardiovascular risk in high-risk hypertensive patients: a subanalysis of the CASE-J Ex.* European Heart Journal, 2012. **33**: p. 760-760.
47. Fukai, T., et al., *Extracellular superoxide dismutase and cardiovascular disease.* Cardiovasc Res, 2002. **55**(2): p. 239-49.
48. Stralin, P., et al., *The interstitium of the human arterial wall contains very large amounts of extracellular superoxide dismutase.* Arterioscler Thromb Vasc Biol, 1995. **15**(11): p. 2032-6.
49. Tsutsui, H., S. Kinugawa, and S. Matsushima, *Oxidative stress and heart failure.* Am J Physiol Heart Circ Physiol, 2011. **301**(6): p. H2181-90.
50. Eto, M., et al., *A novel electron paramagnetic resonance spin-probe technique demonstrates the relation between the production of hydroxyl radicals and ischemia-reperfusion injury.* Eur J Cardiothorac Surg, 2011. **39**(4): p. 465-70.

51. Perron, N.R. and J.L. Brumaghim, *A review of the antioxidant mechanisms of polyphenol compounds related to iron binding.* Cell Biochem Biophys, 2009. **53**(2): p. 75-100.
52. Forgione, M.A., et al., *Heterozygous cellular glutathione peroxidase deficiency in the mouse: abnormalities in vascular and cardiac function and structure.* Circulation, 2002. **106**(9): p. 1154-8.
53. Lubos, E., J. Loscalzo, and D.E. Handy, *Glutathione peroxidase-1 in health and disease: from molecular mechanisms to therapeutic opportunities.* Antioxid Redox Signal, 2011. **15**(7): p. 1957-97.
54. Stone, J.R., *An assessment of proposed mechanisms for sensing hydrogen peroxide in mammalian systems.* Arch Biochem Biophys, 2004. **422**(2): p. 119-24.
55. Noeman, S.A., H.E. Hamooda, and A.A. Baalash, *Biochemical study of oxidative stress markers in the liver, kidney and heart of high fat diet induced obesity in rats.* Diabetol Metab Syndr, 2011. **3**(1): p. 17.
56. McMichael, M.A., *Oxidative stress, antioxidants, and assessment of oxidative stress in dogs and cats.* J Am Vet Med Assoc, 2007. **231**(5): p. 714-20.
57. Cutler, R.G., et al., *Oxidative stress profiling: part II. Theory, technology, and practice.* Ann N Y Acad Sci, 2005. **1055**: p. 136-58.
58. Frye, R.A., *Phylogenetic classification of prokaryotic and eukaryotic Sir2-like proteins.* Biochem Biophys Res Commun, 2000. **273**(2): p. 793-8.
59. Tissenbaum, H.A. and L. Guarente, *Increased dosage of a sir-2 gene extends lifespan in Caenorhabditis elegans.* Nature, 2001. **410**(6825): p. 227-30.
60. Caito, S., et al., *SIRT1 is a redox-sensitive deacetylase that is post-translationally modified by oxidants and carbonyl stress.* FASEB J, 2010. **24**(9): p. 3145-59.
61. Brunet, A., et al., *Stress-dependent regulation of FOXO transcription factors by the SIRT1 deacetylase.* Science, 2004. **303**(5666): p. 2011-5.
62. Wang, F., et al., *SIRT2 deacetylates FOXO3a in response to oxidative stress and caloric restriction.* Aging Cell, 2007. **6**(4): p. 505-14.
63. Hasegawa, K., et al., *Sirt1 protects against oxidative stress-induced renal tubular cell apoptosis by the bidirectional regulation of catalase expression.* Biochem Biophys Res Commun, 2008. **372**(1): p. 51-6.
64. Ahn, B.H., et al., *A role for the mitochondrial deacetylase Sirt3 in regulating energy homeostasis.* Proc Natl Acad Sci U S A, 2008. **105**(38): p. 14447-52.
65. Someya, S., et al., *Sirt3 mediates reduction of oxidative damage and prevention of age-related hearing loss under caloric restriction.* Cell, 2010. **143**(5): p. 802-12.
66. Sundaresan, N.R., et al., *Sirt3 blocks the cardiac hypertrophic response by augmenting Foxo3a-dependent antioxidant defense mechanisms in mice.* J Clin Invest, 2009. **119**(9): p. 2758-71.
67. Maddux, B.A., et al., *Protection against oxidative stress-induced insulin resistance in rat L6 muscle cells by mircomolar concentrations of alpha-lipoic acid.* Diabetes, 2001. **50**(2): p. 404-10.
68. Sorrentino, S.A., et al., *Endothelial-vasoprotective effects of high-density lipoprotein are impaired in patients with type 2 diabetes mellitus but are improved after extended-release niacin therapy.* Circulation, 2010. **121**(1): p. 110-22.

69. Lassegue, B. and R.E. Clempus, *Vascular NAD(P)H oxidases: specific features, expression, and regulation.* Am J Physiol Regul Integr Comp Physiol, 2003. **285**(2): p. R277-97.
70. Touyz, R.M. and E.L. Schiffrin, *Ang II-stimulated superoxide production is mediated via phospholipase D in human vascular smooth muscle cells.* Hypertension, 1999. **34**(4 Pt 2): p. 976-82.
71. Griendling, K.K., et al., *Angiotensin II stimulates NADH and NADPH oxidase activity in cultured vascular smooth muscle cells.* Circ Res, 1994. **74**(6): p. 1141-8.
72. Taniyama, Y. and K.K. Griendling, *Reactive oxygen species in the vasculature: molecular and cellular mechanisms.* Hypertension, 2003. **42**(6): p. 1075-81.
73. Sun, Y.X., et al., *The mechanism of signal transduction during vascular smooth muscle cell proliferation induced by autoantibodies against angiotensin AT1 receptor from hypertension.* Chin Med J (Engl), 2008. **121**(1): p. 43-8.
74. Johar, S., et al., *Aldosterone mediates angiotensin II-induced interstitial cardiac fibrosis via a Nox2-containing NADPH oxidase.* FASEB J, 2006. **20**(9): p. 1546-8.
75. Bell, R.M., et al., *Pivotal role of NOX-2-containing NADPH oxidase in early ischemic preconditioning.* FASEB J, 2005. **19**(14): p. 2037-9.
76. Looi, Y.H., et al., *Involvement of Nox2 NADPH oxidase in adverse cardiac remodeling after myocardial infarction.* Hypertension, 2008. **51**(2): p. 319-25.
77. Sugamura, K. and J.F. Keaney, Jr., *Reactive oxygen species in cardiovascular disease.* Free Radic Biol Med, 2011. **51**(5): p. 978-92.
78. Li, Y., et al., *Dilated cardiomyopathy and neonatal lethality in mutant mice lacking manganese superoxide dismutase.* Nat Genet, 1995. **11**(4): p. 376-81.
79. Nojiri, H., et al., *Oxidative stress causes heart failure with impaired mitochondrial respiration.* J Biol Chem, 2006. **281**(44): p. 33789-801.
80. Furukawa, S., et al., *Increased oxidative stress in obesity and its impact on metabolic syndrome.* J Clin Invest, 2004. **114**(12): p. 1752-61.
81. Keaney, J.F., Jr., et al., *Obesity and systemic oxidative stress: clinical correlates of oxidative stress in the Framingham Study.* Arterioscler Thromb Vasc Biol, 2003. **23**(3): p. 434-9.
82. Szczepaniak, L.S., et al., *Forgotten but not gone: the rediscovery of fatty heart, the most common unrecognized disease in America.* Circ Res, 2007. **101**(8): p. 759-67.
83. Tretter, L. and V. Adam-Vizi, *Inhibition of Krebs cycle enzymes by hydrogen peroxide: A key role of [alpha]-ketoglutarate dehydrogenase in limiting NADH production under oxidative stress.* J Neurosci, 2000. **20**(24): p. 8972-9.
84. Morel, D.W., P.E. DiCorleto, and G.M. Chisolm, *Endothelial and smooth muscle cells alter low density lipoprotein in vitro by free radical oxidation.* Arteriosclerosis, 1984. **4**(4): p. 357-64.
85. Wang, H.T., et al., *Effect of obesity reduction on preservation of heart function and attenuation of left ventricular remodeling, oxidative stress and inflammation in obese mice.* J Transl Med, 2012. **10**(1): p. 145.
86. Orasanu, G. and J. Plutzky, *The pathologic continuum of diabetic vascular disease.* J Am Coll Cardiol, 2009. **53**(5 Suppl): p. S35-42.

87. Roe, N.D., D.P. Thomas, and J. Ren, *Inhibition of NADPH oxidase alleviates experimental diabetes-induced myocardial contractile dysfunction.* Diabetes Obes Metab, 2011. **13**(5): p. 465-73.
88. Scherer, P.E., et al., *A novel serum protein similar to C1q, produced exclusively in adipocytes.* J Biol Chem, 1995. **270**(45): p. 26746-9.
89. Trujillo, M.E. and P.E. Scherer, *Adiponectin--journey from an adipocyte secretory protein to biomarker of the metabolic syndrome.* J Intern Med, 2005. **257**(2): p. 167-75.
90. Ouchi, N., et al., *Novel modulator for endothelial adhesion molecules: adipocyte-derived plasma protein adiponectin.* Circulation, 1999. **100**(25): p. 2473-6.
91. Hotta, K., et al., *Plasma concentrations of a novel, adipose-specific protein, adiponectin, in type 2 diabetic patients.* Arterioscler Thromb Vasc Biol, 2000. **20**(6): p. 1595-9.
92. Tschritter, O., et al., *Plasma adiponectin concentrations predict insulin sensitivity of both glucose and lipid metabolism.* Diabetes, 2003. **52**(2): p. 239-43.
93. Maeda, N., et al., *PPARgamma ligands increase expression and plasma concentrations of adiponectin, an adipose-derived protein.* Diabetes, 2001. **50**(9): p. 2094-9.
94. Qiang, L., H. Wang, and S.R. Farmer, *Adiponectin secretion is regulated by SIRT1 and the endoplasmic reticulum oxidoreductase Ero1-L alpha.* Mol Cell Biol, 2007. **27**(13): p. 4698-707.
95. He, W., et al., *Adipose-specific peroxisome proliferator-activated receptor gamma knockout causes insulin resistance in fat and liver but not in muscle.* Proc Natl Acad Sci U S A, 2003. **100**(26): p. 15712-7.
96. Liu, M., et al., *A disulfide-bond A oxidoreductase-like protein (DsbA-L) regulates adiponectin multimerization.* Proc Natl Acad Sci U S A, 2008. **105**(47): p. 18302-7.
97. Hug, C., et al., *T-cadherin is a receptor for hexameric and high-molecular-weight forms of Acrp30/adiponectin.* Proc Natl Acad Sci U S A, 2004. **101**(28): p. 10308-13.
98. Yamauchi, T., et al., *Cloning of adiponectin receptors that mediate antidiabetic metabolic effects.* Nature, 2003. **423**(6941): p. 762-9.
99. Cohen, S.S., et al., *ADIPOQ, ADIPOR1, and ADIPOR1 polymorphisms in relation to serum adiponectin levels and BMI in black and white women.* Obesity (Silver Spring), 2011. **19**(10): p. 2053-62.
100. Guo, Z., et al., *Cardiac expression of adiponectin and its receptors in streptozotocin-induced diabetic rats.* Metabolism, 2007. **56**(10): p. 1363-71.
101. Sun, X., et al., *Negative regulation of adiponectin receptor 1 promoter by insulin via a repressive nuclear inhibitory protein element.* FEBS Lett, 2008. **582**(23-24): p. 3401-7.
102. Denzel, M.S., et al., *T-cadherin is critical for adiponectin-mediated cardioprotection in mice.* J Clin Invest, 2010. **120**(12): p. 4342-52.
103. Dadson, K., Y. Liu, and G. Sweeney, *Adiponectin action: a combination of endocrine and autocrine/paracrine effects.* Front Endocrinol (Lausanne), 2011. **2**: p. 62.

104. Hamilton, M.P., et al., *Adiponectin and cardiovascular risk profile in patients with type 2 diabetes mellitus: parameters associated with adiponectin complex distribution.* Diab Vasc Dis Res, 2011. **8**(3): p. 190-4.
105. Park, M., et al., *Globular adiponectin, acting via AdipoR1/APPL1, protects H9c2 cells from hypoxia/reoxygenation-induced apoptosis.* PLoS One, 2011. **6**(4): p. e19143.
106. Shinmura, K., *Is adiponectin a bystander or a mediator in heart failure? The tangled thread of a good-natured adipokine in aging and cardiovascular disease.* Heart Fail Rev, 2010. **15**(5): p. 457-66.
107. O'Shea, K.M., et al., *Effects of adiponectin deficiency on structural and metabolic remodeling in mice subjected to pressure overload.* Am J Physiol Heart Circ Physiol, 2010. **298**(6): p. H1639-45.
108. Nanayakkara, G., et al., *The cardio-protective signaling and mechanisms of adiponectin.* Am J Cardiovasc Dis, 2012. **2**(4): p. 253-66.
109. Heiker, J.T., D. Kosel, and A.G. Beck-Sickinger, *Molecular mechanisms of signal transduction via adiponectin and adiponectin receptors.* Biol Chem, 2010. **391**(9): p. 1005-18.
110. Pineiro, R., et al., *Adiponectin is synthesized and secreted by human and murine cardiomyocytes.* FEBS Lett, 2005. **579**(23): p. 5163-9.
111. Vandesompele, J., et al., *Accurate normalization of real-time quantitative RT-PCR data by geometric averaging of multiple internal control genes.* Genome Biol, 2002. **3**(7): p. RESEARCH0034.
112. Wise, A., et al., *Molecular identification of high and low affinity receptors for nicotinic acid.* J Biol Chem, 2003. **278**(11): p. 9869-74.
113. Luo, S. and N.B. Wehr, *Protein carbonylation: avoiding pitfalls in the 2,4-dinitrophenylhydrazine assay.* Redox Rep, 2009. **14**(4): p. 159-66.
114. Kamanna, V.S. and M.L. Kashyap, *Nicotinic acid (niacin) receptor agonists: will they be useful therapeutic agents?* Am J Cardiol, 2007. **100**(11 A): p. S53-61.